UNIVERSITY OF GAZİANTEP
GRADUATE SCHOOL OF
NATURAL & APPLIED SCIENCES

BOND CHARACTERISTICS BETWEEN HIGH EARLY
STRENGTH ENGINEERED CEMENTITOUS COMPOSITES
AND SUBSTRATES

M. Sc. THESIS
IN
CIVIL ENGINEERING

BY
RANJ KHALID HAMEED HAMEED
NOVEMBER 2013

Bond Characteristics Between High Early Strength Engineered Cementitious Composites and Substrates

M.Sc. Thesis
in
Civil Engineering
University of Gaziantep

Supervisors
Assoc. Prof. Dr. Mustafa ŞAHMARAN
Prof. Dr. Mustafa GÜNAL

by
Ranj Khalid Hameed Hameed
November 2013

T.C.
UNIVERSITY OF GAZİANTEP
GRADUATE SCHOOL OF
NATURAL & APPLIED SCIENCES
CIVIL ENGINEERING DEPARTMENT

Name of the thesis: Bond Characteristics Between High Early Strength Engineered Cementitious Composites and Substrates
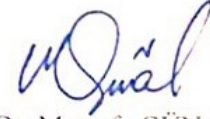
Name of the student: Ranj Khalid Hameed HAMEED
Exam date: November 19, 2013

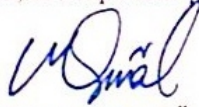Approval of the Graduate School of Natural and Applied Sciences

Assoc. Prof. Dr. Metin BEDİR
Director

I certify that this thesis satisfies all the requirements as a thesis for the degree of Master of Science.
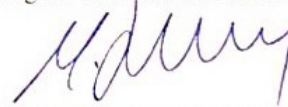
Prof. Dr. Mustafa GÜNAL
Head of Department

This is to certify that we have read this thesis and that in our opinion it is fully adequate, in scope and quality, as a thesis for the degree of Master of Science.

Prof. Dr. Mustafa GÜNAL
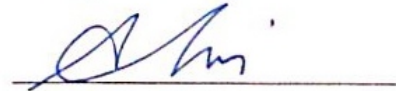Co-Supervisor

Assoc. Prof. Dr. Mustafa ŞAHMARAN
Supervisor
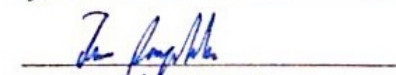
Examining Committee Members   Signature

Assoc. Prof. Dr. Aytaç GÜVEN

Assist. Prof. Dr. Ömer PAYDAK

Assoc. Prof. Dr. Mustafa ŞAHMARAN

I hereby declare that all information in this document has been obtained and presented in accordance with academic rules and ethical conduct. I also declare that, as required by these rules and conduct, I have fully cited and referenced all material and results that are not original to this work.

Ranj Khalid Hameed HAMEED

ABSTRACT

BOND CHARACTERISTICS BETWEEN HIGH EARLY STRENGTH ENGINEERED CEMENTITIOUS COMPOSITES AND SUBSTRATES

HAMEED, Ranj Khalid Hameed
M.Sc. in Civil Engineering
Supervisor: Assoc. Prof. Dr. Mustafa ŞAHMARAN
November2013, 64 pages

An experimental study was undertaken to assess the bond characteristics of High Early Strength Engineered Cementitious Composites – HES-ECC combining very high early strength, high ductility and low early age shrinkage. To do this, composites with different water to cementitious materials and slag to Portland cement ratios were produced. With the purpose of enhancing composite properties in terms of ductility and early age shrinkage characteristics, pre-soaked lightweight aggregates (LWA) were incorporated in some of the HES-ECC mixtures. In addition to HES-ECCs, a mixture of repair material (REPM) which is commercially available and extensively used for fast and durable repair of infrastructures was produced to compare the bonding performance. For the evaluation of bond characteristics on specified days, slant shear and tensile pull-off tests were performed. Along with the basic mechanical properties of proposed materials, influence of compressive strength and differential shrinkage on individual bond strength results was also discussed. Finally, comparison has been made between the results obtained from slant shear and tensile pull-off tests. The experimental results indicate that the influence of compressive strength and differential shrinkage on bond strength results varies significantly depending on the preferred test type. Furthermore, the usage of HES-ECC mixtures significantly improves the bond characteristics of a repair assembly in comparison to REPM. Enhanced bond performance of HES-ECC mixtures over REPMs can more visibly be seen in the case of direct pull-off tests.

Keywords: High-Early-Strength-Engineered Cementitious Composites (HES-ECC); Bond strength; Slant shear test; Direct pull-off test; Mechanical properties.

ÖZET

ERKEN YAŞ YÜKSEK DAYANIMLI ÇİMENTO ESASLI KOMPOZİTLER İLE ALTTABAKA BETONU ARASINDA OLUŞAN BAĞ ÖZELLİKLERİ

HAMEED, Ranj Khalid Hameed
İnşaat Mühendisliği Yüksek Lisans
TezYöneticisi: Doç. Dr. Mustafa ŞAHMARAN
Kasım 2013, 64sayfa

Bu çalışmada yüksek erken yaş dayanımı, yüksek süneklik ve düşük erken yaş rötresi gibi özellikleri bir arada bulunduran Erken Yaş Yüksek Dayanımlı Tasarlanmış Çimento Esaslı Kompozitlerin – HES-ECC bağ özelliklerideğerlendirilmiştir. Bu amaç doğrultusunda, farklı su – bağlayıcı malzeme ve cüruf – Portland çimentosu oranına sahip kompozit malzemeler üretilmiştir. Kompozit özelliklerinin süneklik ve erken yaş rötresi gibi özellikler bakımından iyileştirilebilmesi için, bazı HES-ECC karışımlarında suya doygun hafif agregalar (HA) kullanılmıştır. Bağ özelliklerinin karşılaştırılabilmesi için HES-ECC karışımlarına ek olarak, piyasada yaygın olarak kullanılan bir onarım malzemesi (OM) de üretilmiştir. Bağ özelliklerinin değerlendirilebilmesi için eğik kesme ve çekip koparma testleri gerçekleştirilmiştir. Üretilen malzemelerin temel mekanik özelliklerine ek olarak, basınç dayanımı ve genel rötre oluşumunun bağ dayanımı sonuçları üzerindeki etkileri de tartışılmıştır. Sonuç olarak, eğik kesme ve çekip koparma deneylerinden elde edilen sonuçlar arasında karşılaştırma yapılmıştır. Deneysel sonuçlar basınç dayanımı ve rötre oluşumunun, bağ dayanımı sonuçları üzerindeki etkilerinin kullanılan test yöntemine bağlı olarak önemli ölçüde değiştiğini göstermektedir. Ayrıca, OM'ye oranla, HES-ECC kullanımının bağ özelliklerini önemli ölçüde iyileştirdiği görülmüştür. HES-ECC karışımlarının OM karışımlarına kıyasla gösterdikleri yüksek bağ performansı, hem bağ dayanımı sonuçları hem de kopma tipleri göz önünde bulundurulduğunda çekip koparma testlerinde daha belirgin olarak görülebilmektedir.

Anahtar Kelimeler: Erken Yaş Yüksek Dayanımlı Tasarlanmış Çimento Esaslı Kompozitler (HES-ECC); Bağ dayanımı; Çekip koparma testi; Mekanik özellikler.

ACKNOWLEDGEMENT

TABLE OF CONTENTS

Page

LIST OF FIGURES

LIST OF TABLES

LIST OF SYMBOLS/ABBREVIATIONS

P_Q Applied load

$f\left(\dfrac{a}{W}\right)$ Geometric calibration factor

C   Portland cement

ECC   Engineered cementitious composites

$e^{f\phi}$ Accounts for the changes in bridging force for fibers crossing at an inclined angle to the crack plane

f   Snubbing coefficient

FRC   Fiber reinforced concrete

HES-ECC   High early strength engineered cementitious composites

HRWRA   High range water reducing admixture

J'_b Complimentary energy

J_{tip} Fracture energy of the mortar matrix

K_m Fracture toughness of the mortar matrix

L_f Fiber length

LVDT   Linear variable displacement transducer

LWA   Light weight aggregate

MAS   Maximum aggregate size

p(z)   Centroidal distance from the crack plane

P(δ)	Pullout load versus displacement relation of a single fiber aligned normal to the crack plane
p(ϕ)	Probability density functions of the fiber orientation angle
PVA	Poly-vinyl-alcohol
REPM	Repair material
S	Ground granulated blast furnace slag
S/C	Slag to cement ratio
SEM	Scanning electron microscopy
SUBC	Substrate concrete
V_f	Fiber volume fraction
W/CM	Water to cementitious materials ratio
z	Centroidal distance of a fiber from the crack plane
δ_0	Crack opening
ϕ	Orientation angle of the fiber
σ_0	Maximum crack bridging stress
σ_{fc}	First cracking strength of the mortar matrix

CHAPTER 1

INTRODUCTION

1.1 General

Nations are suffering from early and premature failure of concrete structures since emerging problems endanger the public safety and escalate the necessary cost for repair and/or maintenance which causes significant amount of savings to be burdened. One efficient way to confront this ever-lasting problem is to keep the structures as functional as possible by lowering the frequency of interventions related to repair applications. Although, variety of repair materials that were widely used in the field reported to be adequately durable, the performance of concrete repairs is not always stable (Emmons, 1994; Russell, 2004) and nearly half of the repairs incorporating traditional concrete materials fail in service (Mather and Warner, 2004). Therefore, introduction of concrete repairs addressing the deterioration problems of underlying materials and satisfying durability requirements even in severe environmental conditions is a challenge especially in the case of infrastructures that are more frequently subjected to overloading conditions such as bridge decks, highway pavements, parking structures, and airport runways.

Several papers have concluded that repair materials should meet certain characteristics to be regarded as "ideal". Such characteristics might be listed as the attainment of early age strength in limited time, low early age shrinkage, high ductility and sufficient bond strength with the underlying substratum (Li and Li, 2011; Sahmaran et al., 2013; Parker and Shoemaker, 1991). Among all, maybe the most important parameter is to obtain adequate bond characteristics with the substrate material which could lead the repaired system to behave as one. It should be emphasized that the performance of any repaired installation is only as good as the weakest section of the system which is regarded as the bond formed between the

new and old materials in many instances. In the cases where repaired systems are exposed to excessive loading, the stress concentration will be accumulated either in repair material, substrate or the interface between them. The place where this stress accumulation will occur is dependent on the ability of planes to resist against the stresses. When a failure type which partially extends to all the planes mentioned above is observed, one can understand that repair system is adequately optimized for good bond strength and the material performs well as a repair. It is thus of great importance that during the design of a repair system, the compatibility of individual systems should be accounted for and special attention must be paid for critical planes (e.g. interface).

Although, materials and techniques in great variety were utilized to meet the demand for rapid, inexpensive and durable repairs, only few of them counteracts the drawbacks caused due to quasi-brittle nature of conventional concrete materials (Li, 2009). One of such materials is called as Engineered Cementitious Composites (ECC). ECC is a special type of high performance fiber-reinforced cementitious composite featuring high ductility and damage tolerance under mechanical loading, including tensile and shear loadings (Li, 1997; Li, 2003). With the employment of micromechanics-based material optimization, tensile strain capacity in excess of 3% under uniaxial tensile loading can be attained with only 2% fiber content by volume (Li, 1997; Lin and Li, 1997; Lin et al., 1999). Strain-hardening behavior, which is one of the material characteristics of ECC, is associated with the multiple tight cracking phenomenon of the brittle matrix. The formation of multiple microcracks with the widths of less than 100 m is an intrinsic material property of ECC. This phenomenon is self-controlled and not dependent on the reinforcement ratio. According to Kamada and Li (2000), Lim and Li (1997) and Zhang and Li (2002), ECC can be put to use extensively as a repair layer over existing concrete substrate. It has been reported that compared to conventional concrete and fiber reinforced concrete (FRC) overlays, ECC repair overlays significantly improve the load carrying capacity and ductility of system (Qian, 2007). Additionally, Yucel et al. (2013) and Zhang and Li (2002) stated that the utilization of ECC overlays eliminates common failure types of delamination and reflective cracking in repaired systems.

As previously mentioned, ideal repair material must guarantee the attainment of specific characteristics to serve efficiently in the field. However, despite the best efforts, only a few of the studies aim at combining the necessary characteristics (Wang and Li, 2006; Seehra et al., 1993; Knofel and Wang, 1994; Sprinkel, 1998; Li and Li; 2011). Moreover, to the best of authors, the development of bond strength between this sort of "ideal" repair materials and the substrate where they are applied over is extremely lacking in the literature. Along these lines, in this study, bond performance of High Early Strength Engineered Cementitious Composites –HES-ECC which could be regarded as rather efficient repair material was investigated.

1.2 Research Objectives

Throughout the present study, the bond characteristics of newly developed HES-ECC mixtures which are able to show high strength attainment in limited time, superior ductility and low early age shrinkage formation was discussed. With this purpose in mind, three HES-ECC mixtures with different ground granulated blast furnace slag (S) to Portland cement (C) ratio (S/C) and water to cementitious material ratio (W/CM) were produced. In some of the mixtures, pre-soaked expanded perlite was used as saturated lightweight aggregates (LWA) to optimize ductility by incorporating artificial flaws into the matrix and to reduce early age shrinkage due to increased paste maturity which of both may significantly influence the formation of adequate bond between HES-ECC specimens and substrate concrete. In addition to HES-ECC mixtures, a mixture of repair material (REPM) that is extensively used and can easily be found in the market was cast to compare the results as well. During the experimental work, the development of bond strength was evaluated by tensile pull-off and slant shear tests and comparison has been made between the results obtained from both tests. Additionally, the relationship between compressive strength development and the two different bond tests were presented along with the influence of overall differential shrinkage development values on the results.

In Chapter 2, a detailed literature review on subjects related to the main idea of the present thesis was given. In Chapter 3, experimental program, properties of the materials and details of the tests performed to assess the bond characteristics of proposed materials were presented. The results of the experimental studies are

presented and discussed in Chapter 4. The conclusions of the research are represented in Chapter 5.

CHAPTER 2

LITERATURE REVIEW AND BACKGROUND

2.1 Introduction

Infrastructures such as highways and bridges are in wide use which makes them to be exposed to inevitable heavy overloading conditions and frequent environmental contaminations. The mechanisms leading to deterioration are exacerbated with the usage of de-icing salts during winter seasons which can lead the corrosion of embedded reinforcing bars and eventually internal corruption of concrete material itself. One effective way for slowing down the deterioration mechanisms is the application of protective covers over the existing surfaces which are named as overlays in the literature. An overlay is generally preferred to prolong the service life of the infrastructure by preventing the penetration of water and aggressive agents into the repaired system. It also provides a smooth riding surface, abrasion resistance and reduced thermal movement of the system. The overlay system must also have a compatible load carrying capacity with the substrate materials where they are applied over. The stated requirements can be satisfied when the proposed overlay material reaches to an optimal strength and resists against crack propagation. For economical and highly durable overlay materials, the design and quality control are of critical importance. Increased durability can be ensured by improving free cracking and high bond strength. Moreover, improved skid resistance supplied through thin concrete overlays can have significant influence on the safety of repair assembly.

The usage of rigid pavements is gaining increasing popularity for places exposed to moderate and/or high levels of traffic loads such as bridge decks, highways, airport pavements and industrial floors since these materials can withstand high levels of loads and require low maintenance in comparison to asphalt concrete pavements (Zhang and Li, 2002). During the past decades, several hundred thousand kilometers

5

of rigid pavements were constructed. However, it has been reported that most of the previously built concrete pavements are close to the end of their service life or they require urgent repair (Emmanuel et al., 1998). The usage of different types of overlays over the deteriorated surfaces is the mostly used rehabilitation technique. Although, the application of overlays is widely used around the world and seems like a good solution for the pavement improvement, unresolved questions problems influencing the performance of a repair assembly still exist. Among all, formation of adequate bond between the new overlay material and substratum where they are applied on might be regarded as the most important parameter that affects the performance of the repaired system (Ali and Ambalavanan, 1999; Oluokun and Haghayeghi, 1998; Souza and Appleton, 1997). Attainment of good bond characteristics is vital for successful repair applications. It has been reported that underneath of nearly 10% of the repaired sections over some of bridge decks were found to be empty after a one year (Uherkovich, 1994). One year later the value increased to 30-35% levels. Although these faulty sections were then repaired, empty spots were observed again only a week after. Improvement of the durability of repaired sections has attracted many researchers over the years and interface between the newly applied and old substrate material was regarded to be the most vulnerable section in a repair assembly (Li et al., 2001). Along these lines, throughout the present thesis, emphasis was placed on the attainment of superior bond characteristics by improving interface properties through several material suggestions.

2.2 Engineered Cementitious Composites

As a new class of High Performance Fiber Reinforced Cementitious Composites (HPFRCC) materials, Engineered Cementitious Composites (ECC) is a ductile fiber reinforced cementitious composite micromechanically designed to achieve high damage tolerance under severe loading and high durability under normal service conditions (Li, 1998; Li et al., 2001; Li, 2003). The most distinctive characteristic separating ECC from conventional concrete and fiber reinforced concrete (FRC) is an ultimate tensile strain capacity between 3% to 5%, depending on the specific ECC mixture. This strain capacity is realized through the formation of many closely

6

spaced microcracks, allowing for a strain capacity over 300 times that of normal concrete. These cracks, which carry increasing load after formation, allow the material to exhibit strain hardening, similar to many ductile metals.

While the components of ECC may be similar to FRC, the distinctive ECC characteristic of strain hardening through microcracking is achieved through micromechanical tailoring of the components (i.e. cement, aggregate, and fibers) (Li, 1998; Lin et al., 1999; Li et al., 2001; Li, 2003), along with control of the interfacial properties between components. Fracture properties of the cementitious matrix are carefully controlled through mix proportions. Fiber properties, such as strength, modulus of elasticity, and aspect ratio have been customized for use in ECC. The interfacial properties between fiber and matrix have also been optimized in cooperation with the manufacturer for use in this material. Typical mix proportions of ECC using a poly-vinyl-alcohol (PVA) fiber are given in Table 2.1.

Table 2.1 Typical mix design of ECC material

Cement	1.00
Water	0.58
Aggregate	0.80
Fly Ash	1.20
HRWR*	0.013
Fiber (%)	2.00

*HRWR = High range water reducing admixture; all ingredients proportion by weight except for fiber.

While most HPFRCCs rely on a high fiber volume to achieve high performance, ECC uses low amounts, typically 2% by volume, of short, discontinuous fiber. This low fiber volume, along with the common components, allows flexibility in construction execution. To date, ECC materials have been engineered for self-consolidation casting (Kong et al., 2003a), extrusion (Stang and Li, 1999), shotcreting (Kim et al., 2003), and conventional mixing in a gravity mixer or conventional mixing truck (Lepech and Li, 2007).

Figure 2.1 shows a typical uniaxial tensile stress-strain curve of ECC material containing 2% poly-vinyl-alcohol (PVA) fiber (Weimann and Li, 2003). The characteristic strain-hardening behavior after first cracking is accompanied by multiple microcracking. The crack width development during inelastic straining is

also shown in Figure 2.1. Even at ultimate load, the crack width remains smaller than 80 μm. This tight crack width is self-controlled and, whether the composite is used in combination with conventional reinforcement or not, it is a material characteristic independent of rebar reinforcement ratio. In contrast, normal concrete and fiber reinforced concrete rely on steel reinforcement for crack width control. Under severe bending loads, an ECC beam deforms similar to a ductile metal plate through plastic deformation (Figure 2.2). In compression, ECC materials exhibit compressive strengths similar to high strength concrete (e.g. greater than 60 MPa) (Lepech and Li, 2007).
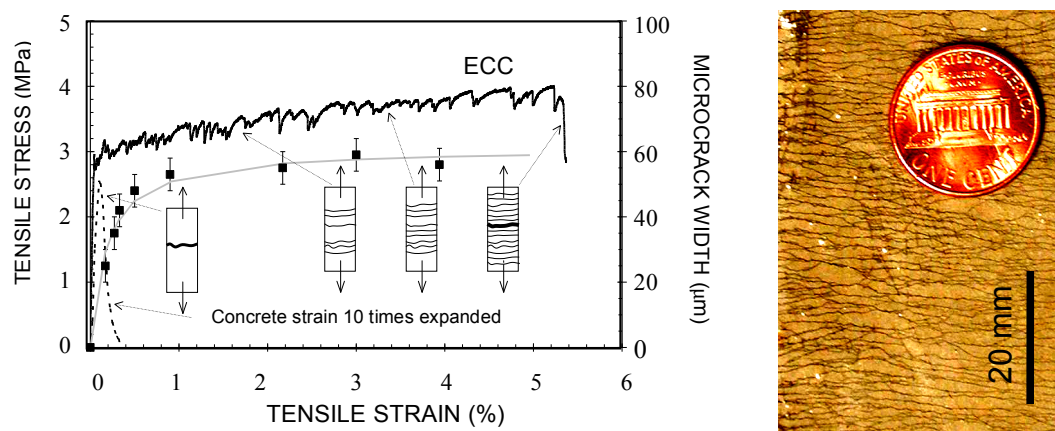
Figure 2.1 Typical tensile stress-strain curve and crack width development of ECC
(Weimann and Li, 2003)
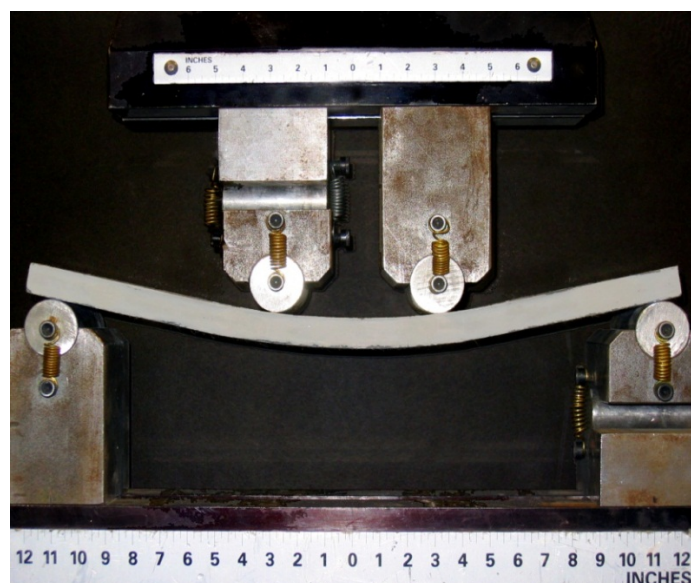
Figure 2.2 Response of ECC under flexural loading

2.3 Design of Engineered Cementitious Composites

In design of ECC material, primary purpose is to assure the occurrence of multiple cracking and strain hardening behavior under loading. Through the formation of multiple microcraks, large deformations are easy to be experienced over the span of specimen. Marshall and Cox (1988) first stated that, the formation of multiple microcraking and strain hardening behavior in ECC is dependent on steady state cracks to propagate. This finding then extended by Li and Leung (1992and Lin et al. (1999) to be used in the case of fiber reinforced cementitious composites. Instead of Griffith-type cracks that open up while propagating as in typical tension-softening fiber reinforced cementitious materials, ECC material experiences large tensile strains in the strain hardening stage through the saturation of specimen with steady state "flat cracks" that keep crack width constant during the propagation. Fiber bridging stress versus crack width opening relation and the cracking toughness of mortar matrix are two main criterions that are responsible for the occurrence of multiple steady state cracking behavior. In order to obtain this behavior the inequality shown in Equation-2.1 must be fulfilled.

$$J_b' = \sigma_0 \delta_0 - \int_0^{\delta_0} \sigma(\delta)d\delta \geq J_{tip} \approx \frac{K_m^2}{E_m} \qquad (2.1)$$

where J'_b is the complimentary energy shown in Figure 2.3, σ_0 and δ_0 are the maximum crack bridging stress and corresponding crack opening, J_{tip} is the fracture energy of the mortar matrix, K_m is the fracture toughness of the mortar matrix, and E_m is the elastic modulus of the mortar matrix. In addition to the fracture energy criterion, a strength criterion expressed in Equation-2.2 must be satisfied.

$$\sigma_0 > \sigma_{fc} \qquad (2.2)$$
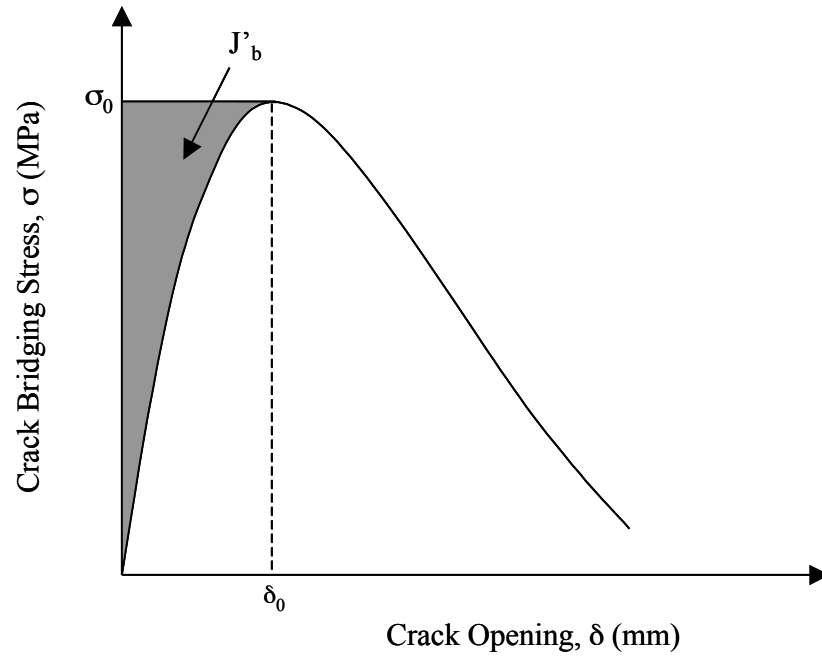
Figure 2.3 Crack bridging stress versus crack opening relation

where, σ_0 is the maximum crack bridging stress and σ_{fc} is the first cracking strength of the mortar matrix. For saturated multiple cracking, Wang and Li (2004) found that Equation-2.2 must be satisfied at each potential crack plane, where σ_{fc} is understood as the cracking stress on that crack plane.

Development of multiple steady state crack formation and strain hardening behavior can be well understood through the attainment of ECC mixture that adequately meets the two abovementioned parameters. However, along with the formation of steady state cracks, the material design must be made to obtain crack widths less than 100 μm threshold limit. This need can be satisfied with the tailoring of crack bridging versus crack opening relation stated in Equation-2.1. As shown in Figure 2.3, during the multiple microcracking of ECC material, the maximum steady state crack width can be regarded as δ_0 and the crack width accounting for the maximum crack bridging stress as σ_0. Crack bridging stress starts to decrease, if crack width exceeds δ_0 value. In this case, localized cracks start to occur and the formation of multiple steady state microcracks ceases. However, as δ_0 value is kept under 100 μm threshold, multiple microcracking and strain hardening behavior can be acquired.

Lin et al. (1999) proposed the formulation of the crack bridging stress versus opening relationship based on summing the bridging force contribution of fibers that cross a given crack plane. This relation in expressed in Equation-2.3.

$$\sigma(\delta) = \frac{4V_f}{\pi d_f^2} \int_{\phi=0}^{\pi/2} \left(\int_{z=0}^{(L_f/2)\cos\phi} P(\delta)e^{f\phi}p(\phi)p(z)dz \right) d\phi \qquad (2.3)$$

where V_f is the fiber volume fraction, d_f is the fiber diameter, ϕ is the orientation angle of the fiber, L_f is the fiber length, z is the centroidal distance of a fiber from the crack plane, f is a snubbing coefficient, and $p(\phi)$ and $p(z)$ are probability density functions of the fiber orientation angle and centroidal distance from the crack plane, respectively. $P(\delta)$ is the pullout load versus displacement relation of a single fiber aligned normal to the crack plane, also described in Lin et al. (1999). The factor $e^{f\phi}$ accounts for the changes in bridging force for fibers crossing at an inclined angle to the crack plane.

Through the use of basic micromechanical models, ECC material can be tailored to endure larger strains up to several percent without the formation of larger cracks that could cause an increase in overall permeability. The application of material design procedures, such as those outlined above, allow materials engineers to carefully match material characteristics to specific structural demands, such as strain capacity and low permeability.

2.4 Factors Influencing Bond Between New and Old Concrete

2.4.1 Compressive Strength

The effect of compressive strength of the overlay materials on the adhesion behavior to an existing substrate concrete was investigated by Julio et al. (2006). In the study, three different types of concrete mixtures having 28-day-old compressive strength values of 30, 50 and 100 MPa (M30, M50 and M100) were produced. The bond strength development of different concrete mixtures was evaluated by slant shear tests. During the tests, three conditions were taken into account as 30/30, 30/50 and 30/100 of which the first value showing the compressive strength of substrate

concrete while the second value showing the 28-day-old compressive strength result of the added concrete mixtures. As a result of the tests it was observed that while all of the 30/30 specimens showed adhesive fracture mode (Figure 2.4-a), all of the 30/50 and 30/100 specimens exhibited monolithic fracture mode (Figure 2.4-b).

(a)   (b)
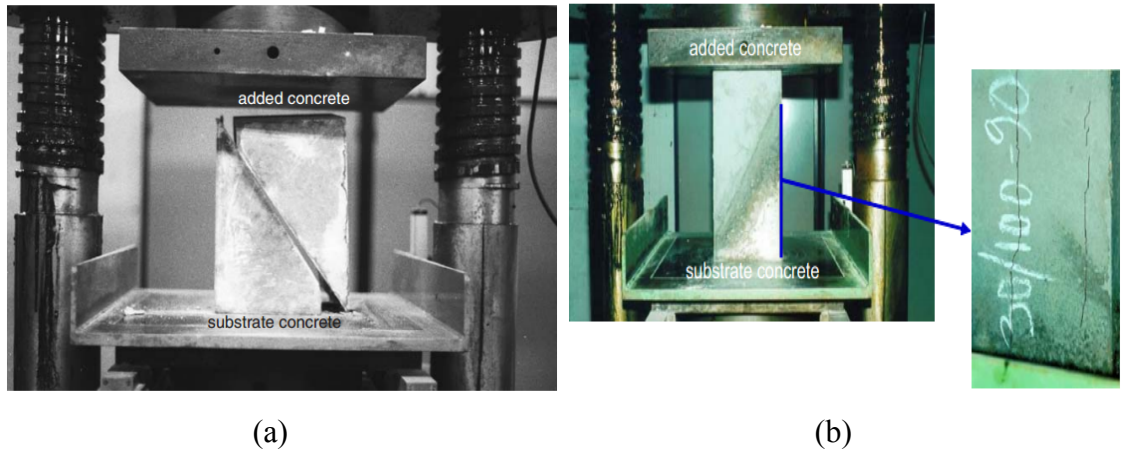
Figure 2.4 Fracture types of a) 30/30 specimens b) 30/50 and 30/100 specimens
(Julio et al., 2006)

In order to understand why specimens with different compressive strengths showed different fracture modes a numerical analysis method using the finite element method was performed. Results of the finite element analysis were shown in Figure 2.5.

(a)   (b)
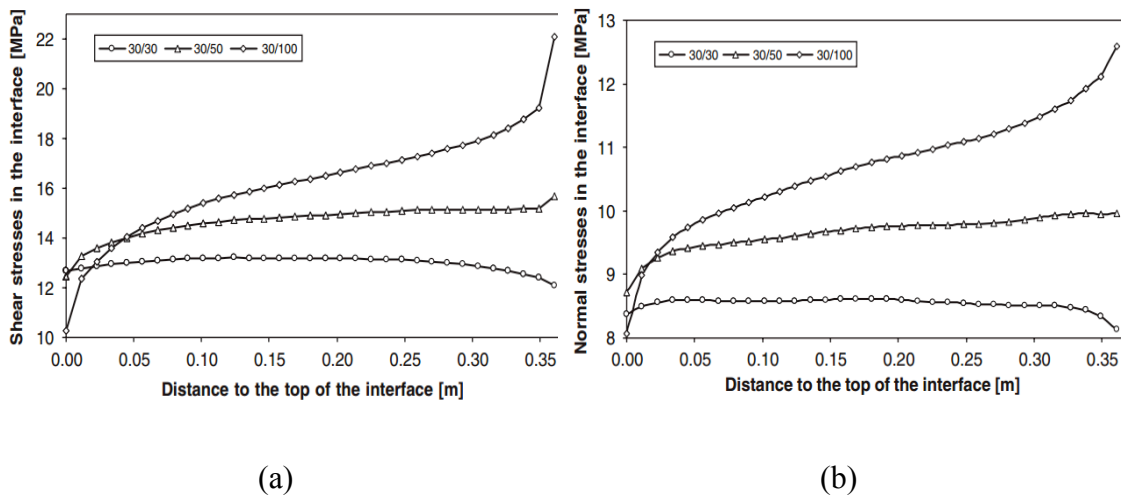
Figure 2.5 Distribution of a) shear stresses b) normal compression stresses in the interface (Julio et al., 2006)

As seen from the figure, in the case of 30/30 specimens, shear stresses at the interface were uniformly distributed. However, when 30/50 specimens were evaluated it can be seen that shear stresses started to create peaks near the top and bottom surfaces of the interface. This behavior was found to be more pronounced in the case of 30/100 specimens. Although the distribution of shear stresses changes depending on the compressive strength results of the added concrete, this finding does not justify the observed fracture modes. In addition to the shear stress formation near the interfaces, the distribution of normal stresses in compression were also shown in Figure 2.5-b. As seen from the figure same modality as in shear stress distribution was observed in the case of distribution of normal stresses in the interface. The observed behavior of normal stress distribution does not account for the different rupture modes of different composite specimens as well. In Figure 2.6, shear stresses were plotted against normal stresses.

Shear stress *versus* normal stress in the interface
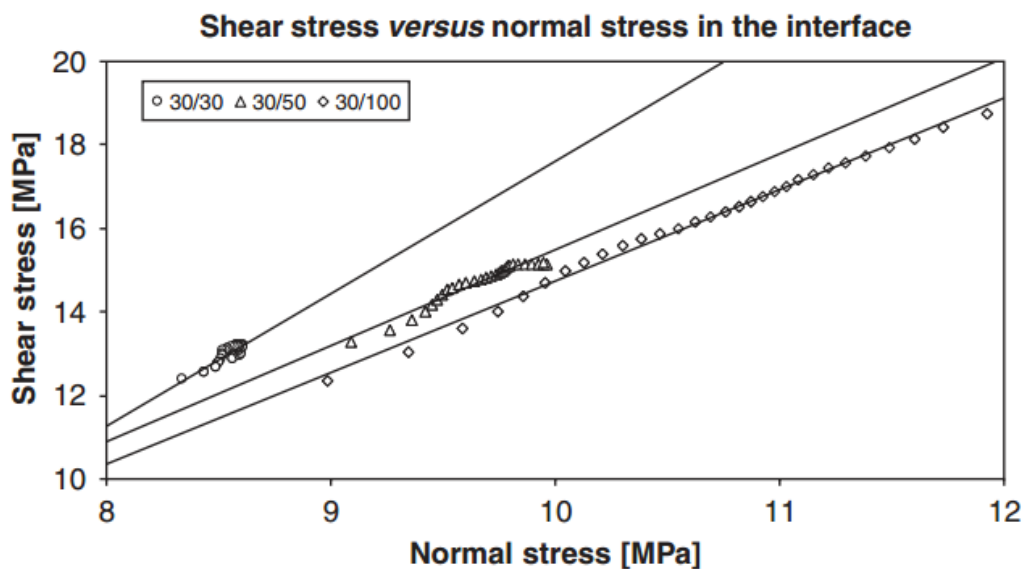
Figure 2.6 Relationship between shear and normal stresses in the interface (Julio et al., 2006)

As it is clear from Figure 2.6 that for a certain shear stress value there is an increase in normal stress development in the interfaces as the strength of added material is increased. This means that with the increase in normal stresses at a constant shear stress value, friction between the two different concrete layers will be increased. This may be the explanation for the changes in rupture modes with the increase change in compressive strength results of the added materials.

In another study undertaken by Beushausen and Alexander (2008), the influence of compressive strength on bond strength development was evaluated through interface shear bond tests (Figure 2.7).

Figure 2.7 Photograph of interface shear bond test method used for short-term bond strength evaluation (Beushausen and Alexander, 2008)

For the evaluation of short-term bond strength development overlay materials named S1, S2, S3 and S4 having 28 day design compressive strength values of 50, 30, 20 and 10 MPa were produced. The overlays were applied on sandblasted substrate surface. The results were given in Figure 2.8.
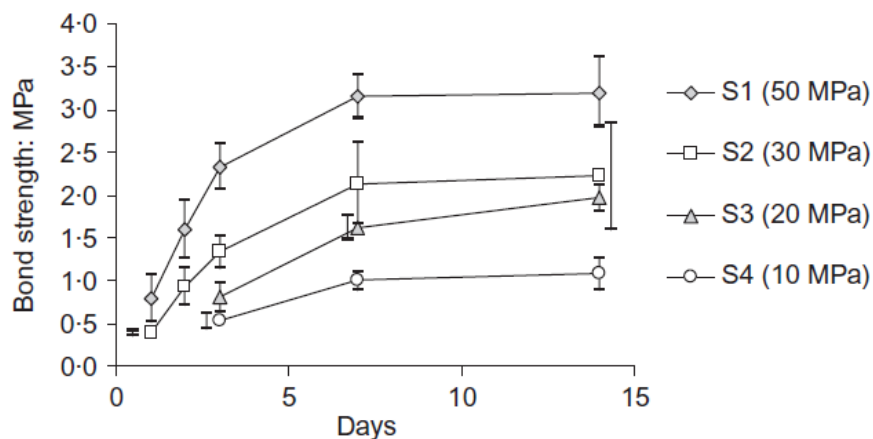
Figure 2.8 Short-term bond strength development of S1-4 specimens (Beushausen and Alexander, 2008)

As seen from the figure, overlay compressive strength significantly affects the final shear bond strength results. Increase in compressive strength resulted in higher bond strength values although the increasing trend lost its intensity in the later ages. It is generally considered that shear failure in concrete is originated due to tensile-like stresses that are perpendicular to the shear plane. Therefore, it can be said that shear strength can be correlated with the tensile strength and indirectly with the compressive strength of concrete. According to Neville (2002), tensile strength increases with a decreasing rate as the compressive strength increases. This thus may be the explanation for the decreasing behavior in shear bond strength results with time despite the increase in compressive strength results.

2.4.2 Differential Shrinkage

Stresses are generated due to differential shrinkage formation between newly applied repair materials and substrate materials. It is of high probability that these stresses may lead to interface delamination and/or cracking in repair material which increases the chance for harmful substances to penetrate to the repair assembly and cause several deteriorating mechanisms such as corrosion of the rebar, sulfate attack etc. The influence of differential shrinkage on interface shear strength results was studied by Beushausen and Alexander (2008). During their study, one type of concrete mixture was applied over substrate concretes having three different surface textures namely sandblasted, smooth and notched (S5, S6 and S7, respectively). Interface shear strength was measured by guillotine test shown in Figure 2.9.

Figure 2.9 Photograph of interface shear bond test method, guillotine test
(Beushausen and Alexander, 2008)
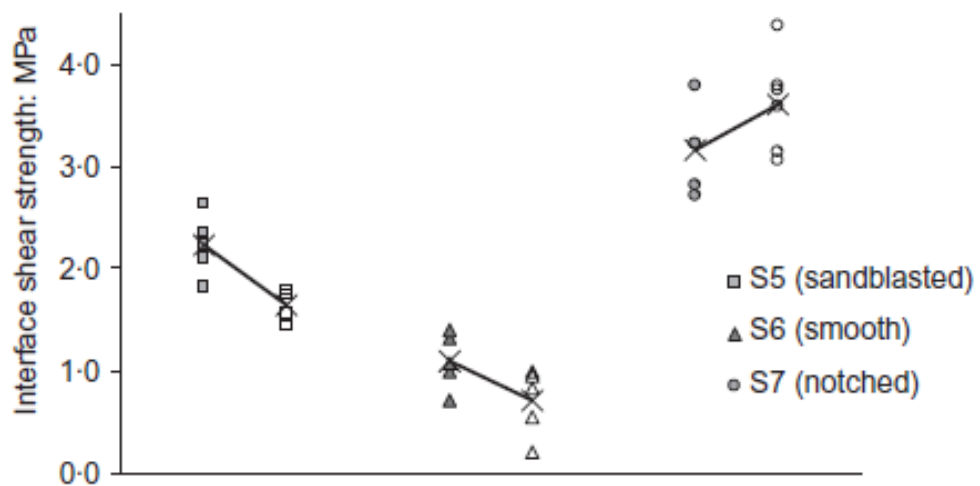
Figure 2.10 Development of interface shear strength under laboratory conditions.
Comparison between results obtained at 28 days (filled symbols) and 26 months
(unfilled symbols) (Beushausen and Alexander, 2008)

As seen from the figure while 26-month-old S5 (sandblasted) and S6 (smooth)
specimens showed nearly 25% of decrease in interface shear strength results
compared to 28-day-old specimens, an opposite behavior was observed in the case of

16

S7 (notched) specimens. In the case of specimens S5 and S6, failure was observed in the places very close to the interface areas. However, notched S7 specimens showed a type of failure extending interface, substrate and overlay areas at the same time. It is interesting to point out that although all the specimens were with the same shrinkage characteristics, only S7 specimens showed an increase in bond strength results between 28 days and 26 months. The reason for this behavior was correlated with the effectiveness of notches in providing mechanical interlocking which caused failure either in overlay or substrate before the affection of interface. Therefore, a big part of shear strength in the case of S7 specimens was found to be in relation with the material shear strength rather than interface shear strength. This finding also suggests that under the influence of differential shrinkage, specimens having macro-roughness show more durable shear bond strength development with respect to specimens having micro-roughness.

In a different study conducted by Santos and Julio (2011) effect of differential shrinkage on slant shear test (the shape of specimens are similar to specimens shown in Figure 2.4) results was examined by a numerical study using finite elements software. Throughout the study, three different time intervals (28, 56 and 84 days) were used between the first time of substrate concrete pouring and the time of casting the new repair materials. Two environmental conditioning were applied to composite specimens one of which is the interior of the laboratory (L28, L56 and L84) and the other is the exterior of the laboratory (E28, E56 and E84). Before the commencement of tests, an experimental shrinkage strain was applied both to the substrate and newly applied materials by taking into account the different time intervals and curing conditions. The results were in line with the previously mentioned study of Beushausen and Alexander (2008) so that with the increase in time intervals which also increases the differential shrinkage both shear and normal stresses showed an increase in results (Figure 2.11).

(a)   (b)
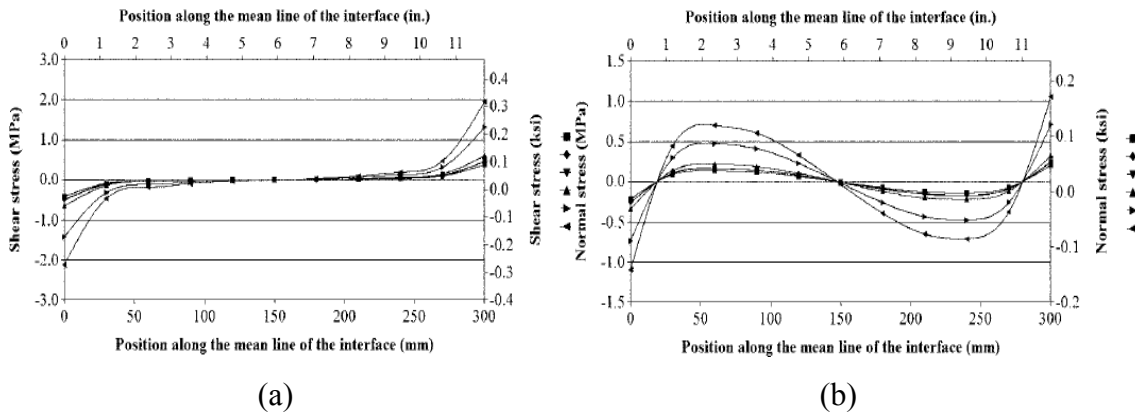
Figure 2.11 Distribution of a) shear b) normal stresses at the interface due to
differential shrinkage (Santos and Julio, 2011)

2.4.3 Modulus Mismatch

It has been reported that significant changes in stiffness values of different concrete
layers lead variations in stress distribution at the interface of a repair assembly. This
topic thus became of interest to many researchers. In their study Santos and Julio
(2011) have focused on the influence of differential shrinkage on stress distributions
at the interface between the added concrete over substrate concrete. In this study, an
experimental work was performed with four different concrete classes (C20/25,
C25/30, C40/50, and C90/105) that were applied over one type of substrate concrete
(C20/25). The elastic moduli of the different concrete types were 30, 31, 35 and 44
GPa, respectively. In Figure 2.12, the shear and normal stress distributions of
different composite systems obtained by finite element system software were
provided.

(a)   **(b)**
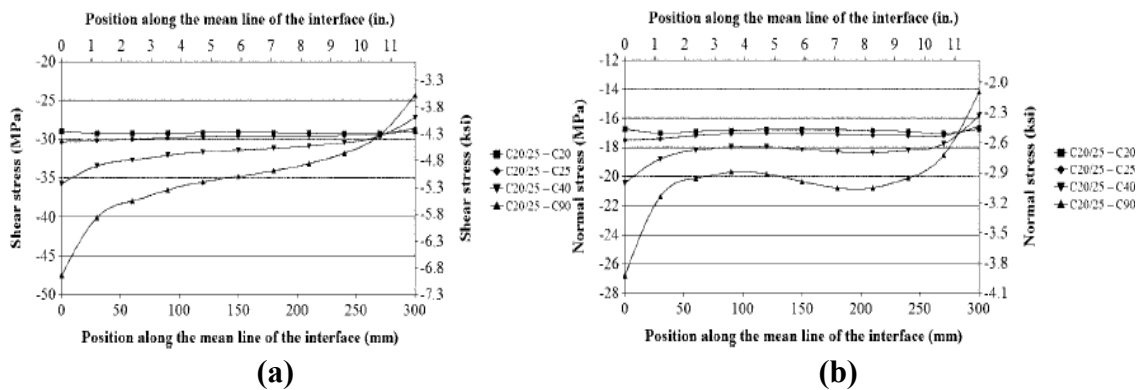
Figure 2.12 Distribution of a) normal b) shear stresses due to differential stiffness
(Santos and Julio, 2011)

As seen from Figure 2.12, the differences in stiffness values of several concrete mixtures substantially affect the distribution of both shear and normal stresses. It can be stated that as the difference between the stiffness values of new and substrate concretes increases stress concentrations form at the both ends of the interfaces and the stresses distribute in an S-shaped form which might serve as an indicator for the different failure types observed throughout the study (Figure 2.13).

(a)   (b)
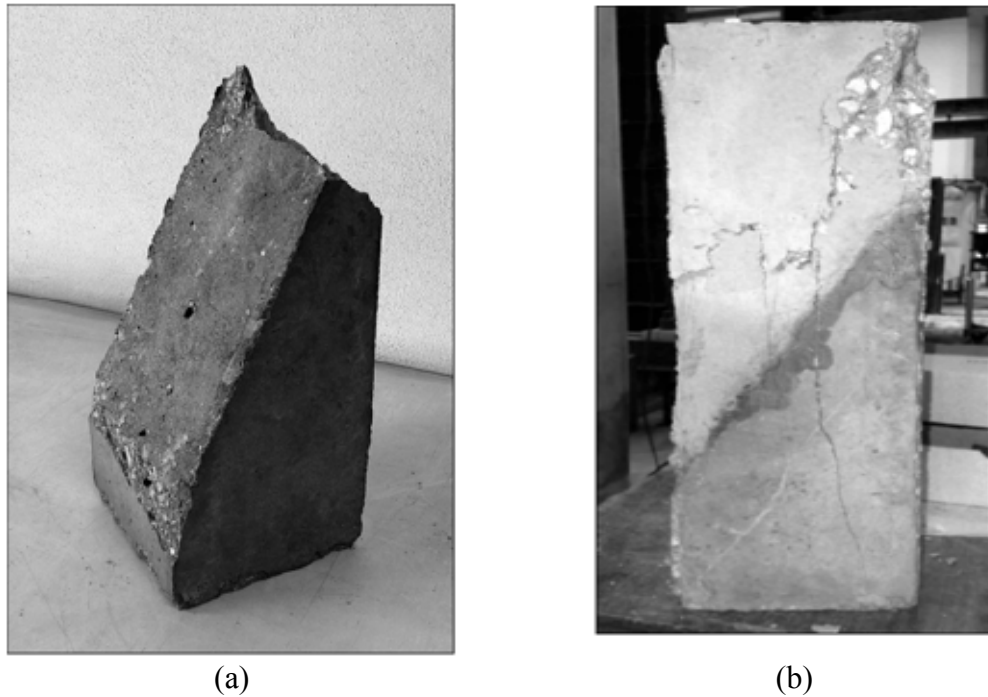
Figure 2.13 Failure modes for slant shear tests a) adhesive, b) cohesive

Hassan et al. (2001) investigated the compatibility of different repair materials with the conventional concrete in terms of modulus of elasticity values. In their study, five different repair materials were applied on a conventional parent concrete. Repair materials included ordinary portland cement (OPC), fly ash mortar (FA), silica fume mortar (SF), polymer modified mortar (PMC) and epoxy resin mortar (EP). Elastic modulus is a material property which has a strong influence on the distribution of stresses in combined repair systems incorporating two different materials. In Figure 2.14 stress-strain relationships for different repair materials were given along with the parent concrete (Conc) and combined systems (Comb). The graphs were drawn up to 1/3 of the final failure load in order to show elastic behavior more clearly.
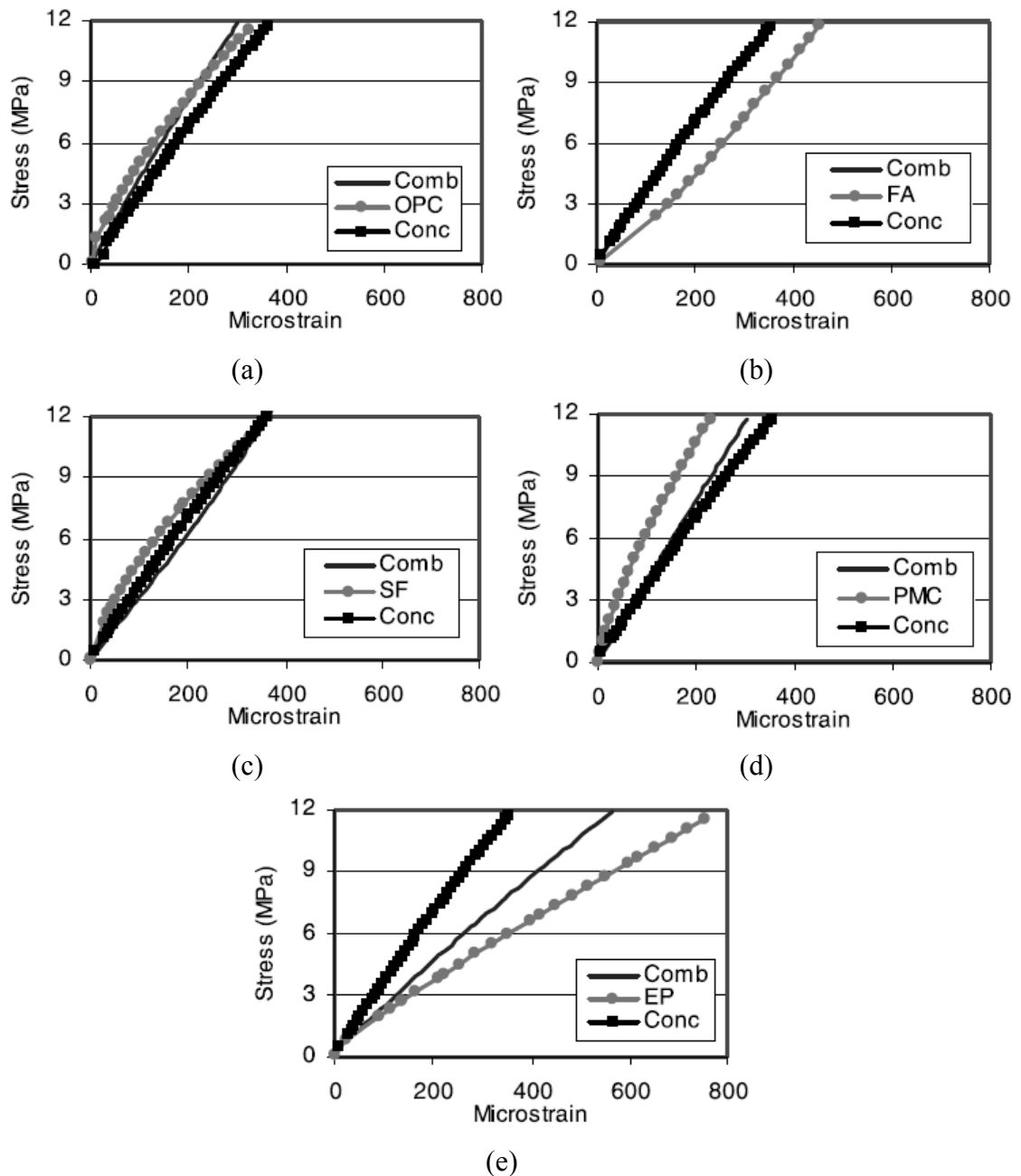
Figure 2.14 Stress-strain relationships for the different combined systems a) OPC/Conc, b) FA/Conc, c) SF/Conc, d) PMC/Conc, and e) EP/Conc (Hassan et al., 2001)

As seen from the figure, excluding those obtained from PMC and EP repairs, modulus values of repair materials are rather similar to the modulus of elasticity of parent concrete. It is also visible from the figure that elastic moduli of combined systems of OPC, FA and SF repairs did not show a significant variation which implies that load distributions and modulus compatibility of the systems were not strongly influenced. In the case of PMC and EP mortars however, there was a high variation in the elastic modulus results showing that the load distribution between the

new and old materials will change with the application and the bond between the materials will be affected negatively.

2.4.4 Substrate Surface Preparation

For a successful repair assembly to be obtained, firstly the substrate concrete must be prepared in a sufficient manner. The attainment of adequate bond characteristics is achievable but if the substrate concrete is not well-prepared, the repair assembly may inevitably fail. There are conflicting arguments in the literature about preparing the substrate concretes in a proper way and vast amounts of different substrate preparation techniques proposed by different authorities over the years.

In the study performed by Tayeh et al. (2012) the bond characteristics of ultra-high performance fiber reinforced concrete (UHPFC) to the normal concrete (NC) were investigated in terms of slant shear and splitting tensile strength tests. During the study five differently roughened substrate surfaces were used for assessment. Five different surface textures prepared were as cast (AC) with no preparation, sand blasted (SB), wire brush (WB), drilled holes (DH) and grooved (GR) (Figure 2.15).
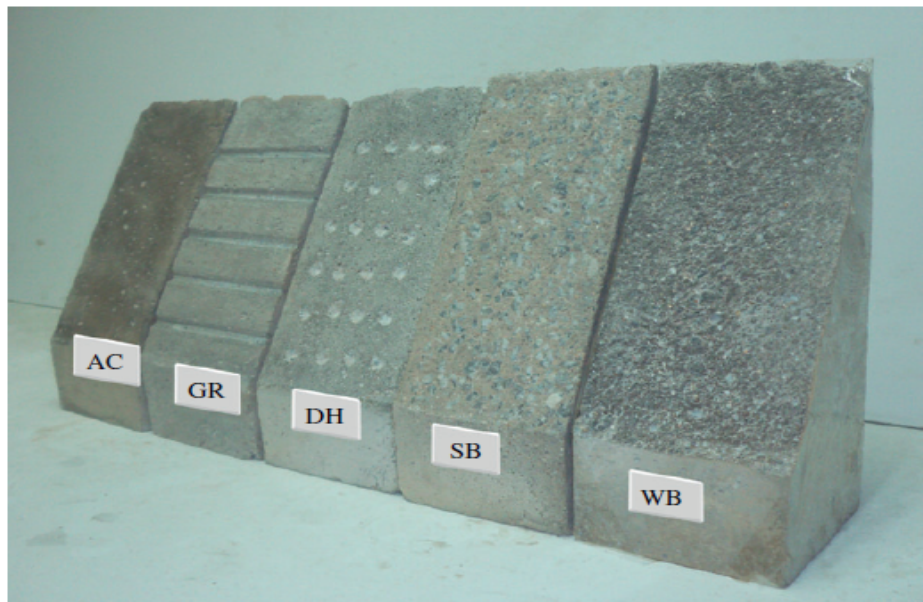
Figure 2.15 Different substrate surface textures (Tayeh et al., 2012)

The bond strength results obtained from the experimental study of both bond tests were shown in Figure 2.16.
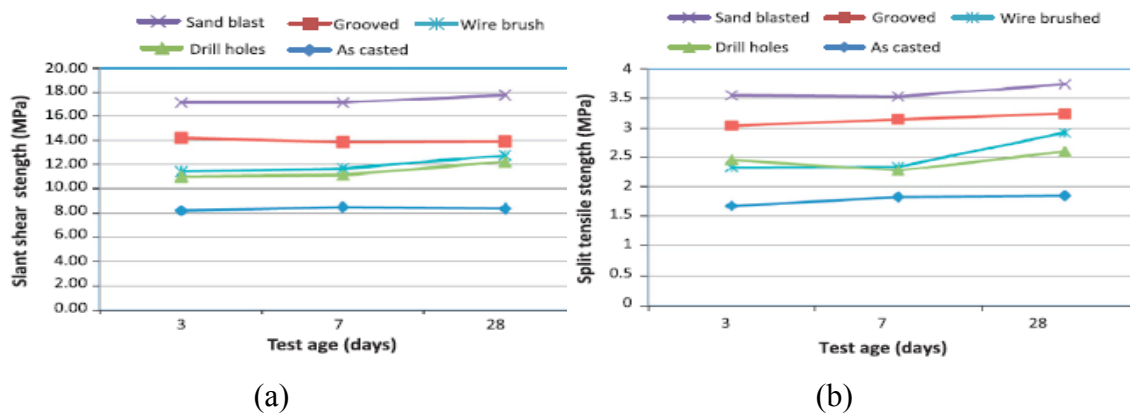
Figure 2.16 Bond strength values obtained with a) slant shear b) splitting tensile tests (Tayeh et al., 2012)

As seen from the figure, regardless of the test technique, the highest bond strength results were obtained from sand blasted specimens. The improvement in both bond strength values was significant with no respect to the type of surface texture. The results showed an increasing trend in time due most probably to the cement hydration and pozzolanic activities of ingredients in UHPFC mixtures which caused enhanced interfacial bonding in time. The reason for the enhancement in both bond strength results with the change in surface textures from smooth to rough can be linked to improved adhesion and interlocking effect. It was also reported that silica fume used during the production of UHPFC mixtures played a major role in improving bond strength results through providing micro-filler effect and substantial pozzolanic activity. Another possible mechanism that might contribute to high bonding capability with the use UHPFC mixtures as overlay could be that after the substrate surfaces were roughened, calcium hydroxide which is ready for immediate pozzolanic activity was provided which created high probability for silica fume particles to react with. This leaded both mechanical and chemical bond simultaneously and enhanced the bonding properties of textured composite specimens compared the specimens having smooth substrates.

2.5 Common Bond Strength Testing Methods

Common bond strength test techniques are composed of interface shear, torsion and tension tests. Over the years many researchers engaged in and applied new test

methods both in laboratory and field conditions to assess the bond strength development. The interfacial bond strength values obtained from different tests can vary significantly since the results are highly dependent on several parameters such as the size of specimen, testing equipment, rate of loading and so on. Setting a correlation between interfacial shear and tension tests is highly arguable since different test methods are strongly influenced by different characteristics as mentioned above. According to Silfwerbrand (2003) and Delatte et al. (2000) however there is a correlation existing between the two test techniques. Delatte et al. (2000) stated that there exist a mean ratio of 2.0 between shear bond results by tension bond results. According to Silfwerbrand (2003), ratio of torsional shear bond strength by tensile pull-off strength is in the range of 2 to 3.

In Figure 2.17, the schematic representations of all of the existing testing methods used during the assessment of bond strength development between different concrete mixtures were provided.
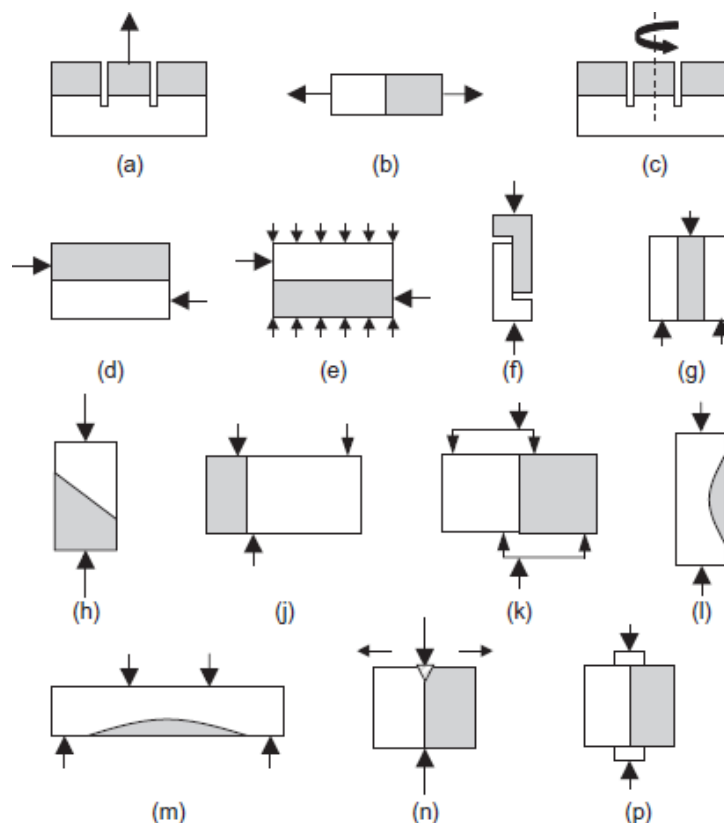
Figure 2.17 Schematic representations of several test techniques for the determination of interfacial bond strength (Silfwerbrand, 2003)

Tensile pull-off test is the most commonly used test technique which can easily be performed both in the field (Figure 2.17-a) and laboratory conditions (Figure 2.17-b). Along with its easiness, the popularity of tensile test techniques can be closely related with the possibility to be easily performed both in the laboratory and in-situ. Despite their popularity however, there are several problems that can be encountered during the tensile pull-off tests one of which is eccentricity that may be exerted during the core drilling process (Delatte et al., 2000-a). It has reported that the tensile pull-off strength test results show great variability which makes final interpretation harder (Delatte et al., 2000-a; USDT, 2000). In the case of overlays that are placed in a proper way and having high bond strength, quantification is hard with the tensile pull-off tests but in the cases where the tensile strength of the tested material is higher than the interface bond strength quantification is easy by the tensile pull-off tests. This thus means that the results obtained through the utilization of tensile pull-off bond test indicate only lower bound of the interfacial bond strength.

A newly developed in situ test for the measurement of torsional bond strength and the results of which can be related to the interfacial shear bond strength was introduced by Silfwerbrand (2003) (Figure 2.17-c). In the case of commonly used shear bond tests generally a force parallel to the interface is applied (Figure 2.17-d). Pigeon and Saucier (1992) and El-Rakib et al. (2003) used modified shear bond methods shown in Figure 2.17-f during their experimental studies. In the case of push-out tests shown in Figure 2.17-g, (Larralde et al., 2001; Momayez et al., 2004; Chen et al., 1995) there are disadvantages related to having two different interfaces and the results obtained does not represent the real field conditions. These make the usage of this technique very impractical. In Figure 2.17-h, slant shear bond strength test combining both shear and compression load application was shown. Although, this test method was preferred by many, some shortcomings were reported related to the loading conditions and large number of factors influencing the final results (Austin et al., 1999; Delatte et al., 2000; Emberson and Mays, 1990). The guillotine test which was shown in Figure 2.7-j can be used both on core and prism specimens. However, it has been stated that there are some difficulties related to the alignment of the loading head during the usage on core specimens (Delatte et al, 2000). One of the most commonly encountered problems during the shear test methods is the interface bending moment caused due to force eccentricity. Along these lines, a test method

which directly subjects the specimens to pure shear forces was developed as seen in Figure 2.17-k (Fe´de´ration Internationale de la Pre´contrainte, 1978). In Figure 2.17-l and 2.17-m, there are different patch tests measuring shear and tensile bond strength under the structural loading conditions were shown (Robins and Austin, 1995). The wedge splitting test device shown in Figure 2.17-n allows the characterization of the bond parameters related to fracture mechanics such as crack opening, specific fracture energy and tensile interface bending strength (Tschegg et al., 2000). In Figure 2.17-p, splitting prism test device measuring the interface tensile strength used by Li et al. (1996) was shown.

CHAPTER 3

EXPERIMENTAL PROGRAM

3.1 Materials

3.1.1 CEM I 42.5R Portland Cement

The cement used during the production of substrate concrete was a normal portland cement CEM I 42.5R, which corresponds to ASTM Type I cement. It had a specific gravity of 3.06 and Blaine fineness of 325 m^2/kg. Chemical composition and physical properties of cement are presented in Table 3.1.

Table 3.1 Chemical and physical properties of different cement types and slag

Chemical Compositions	CEM I 52.5R	CEM I 42.5R	S
CaO	65.7	61.4	35.1
SiO_2	21.6	20.8	37.6
Al_2O_3	4.1	5.6	10.6
Fe_2O_3	0.26	3.4	0.28
MgO	1.3	2.5	7.9
SO_3	3.3	2.5	2.9
K_2O	0.77	0.77	1.1
Na_2O	0.19	0.19	0.24
Loss on Ignition	3.2	2.2	2.8
$SiO_2+Al_2O_3+Fe_2O_3$	25.9	29.8	48.4
Compound compositions			
C_3S	65.2	58. 6	-
C_2S	16.7	17.1	-
C_3A	10.3	6.4	-
C_4AF	0.79	8.8	-
Physical Properties			
Specific Gravity	3.06	3.06	2.8
Blaine Fineness (m^2/kg)	460	325	425

3.1.2 CEM I 52.5R Portland Cement

The cement used during the production of HES-ECC mixtures was a fast setting portland cement CEM I 52.5R, which correspond to TS EN 197-1 CEM I type

cement. It has a Blaine fineness of 460 m^2/kg. Chemical composition and physical properties of cement are presented in Table 3.1.

3.1.3 Slag

Slag (S) was supplied from Iskenderun Iron–Steel Factory in Turkey. Its chemical oxide composition is given in Table 3.1. The specific gravity of slag was 2.79 g/cm^3. Slag was ground granulated in Iskenderun Cement Factory to have a Blaine specific surface area about 425 m^2/kg. According to ASTM C 989 (2009) hydraulic activity index, the slag used was classified as a category 80 slag. To identify morphological characteristics of slag, it was analyzed with SEM and the resulting photograph is presented in Figure 3.1.
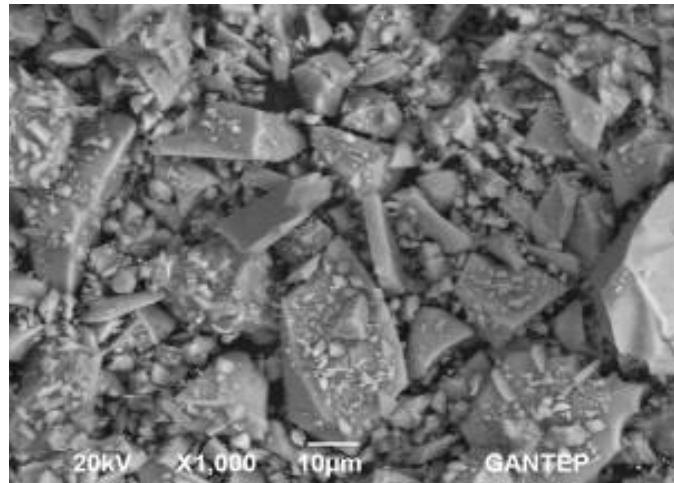
Figure 3.1 Particle morphology of slag determined by SEM

3.1.4 Silica Sand

According to micromechanic-based design of ECC, exhibiting ductile and showing a large crack number, but small in width, of cementitious composites a low fracture toughness of the matrix is required. However, with the increasing of maximum grain size of aggregate, increase in toughness of the matrix is appeared and as a result, to obtain suitable ECC, aggregate grain size is limited (Li et al.,1995).

Therefore, so far, ECC has been produced successfully with an average grain size of about 110 μm (Li et al., 1995). Using high volumes of industrial by-product in the production of ECC decreases matrix fracture toughness and provides freedom of changing aggregate size. It is very important to produce ECC from normal size local

sources of aggregate in terms of widespread application for both literature and our country. For this purpose, in the production of ECC, fine quartz with a nominal aggregate size (MAS) of 400 μm was obtained from local sources in Turkey's resources. Water absorption capacity and specific weight of quartz aggregate used is 0.3% and 2.60, respectively.

3.1.5 Expanded Perlite Lightweight Aggregate

The lightweight aggregate used in this study was expanded perlite type commercially manufactured. The expanded fine perlite (F) which have MAS of 1 to 2 mm used in this study had water absorption capacity of nearly 131% and specific gravity of 0.92. Perlite is a siliceous volcanic glass, the volume of which can expand substantially under the effect of heat. The perlite used consisted mainly of about 75% SiO_2 and 13% Al_2O_3. When heated above 900 °C, its volume increases up to 35 times of the original volume. As a result of this volume increase, absorption of the expanded perlite is significantly high. Moreover, the density of expanded perlite is very low $(850 \pm 25 \text{ kg/m}^3)$.

Figure 3.2 View of expanded perlite aggregate

3.1.6 Chemical Admixtures

To improve the workability of ECC mixtures, Glenium 51, high range water reducing admixture (HRWR – polycarboxylate ether as an active ingredient with 1.1

specific gravity and 40% solid content) produced by BASF Construction Chemicals was used.

Also, calcium nitrate salt based accelerator (Pozzolith 326 B) with the density of 1.316 – 1.376 kg/liter was used to fasten the reactions between water and cement especially when the initial set was reached.

3.1.7 Polyvinyl Alcohol (PVA) Fiber

Although various fiber types have been used in the production of ECC, PVA fiber was used in this study (Figure 3.3).

Figure 3.3 PVA Fiber used in the production of ECC

The use of PVA fiber was decided based on and PVA-ECC represents the most practical ECC used in the field (Li et al., 2001; Kunieda and Rokugo, 2006) at the present. PVA fibers have attracted most attention due to the outstanding composite performance and economics consideration. The dimensions of the PVA fiber are 8 mm in length and 39 μm in diameter. The nominal tensile strength and elastic modulus of the fiber is 1620 MPa and 42,8 GPa respectively and the density of the fiber is 1300 kg/m^3. The mechanical and geometric properties of PVA fibers are summarized in Table 3.2.

Table 3.2 Mechanical and Geometric Properties of PVA Fibers

Fiber Type	Nominal Strength (MPa)	Apparent Strength (MPa)	Diameter (µm)	Length (mm)	Elastic Modulus (GPa)	Ultimate Strain (%)	Specific Weight kg/m^3
PVA	1620	1092	39	8	42.8	6.0	1300

The PVA fiber is surface-coated by hydrophobic oil (1.2% by weight) in order to reduce the fiber/matrix interfacial bond strength. To account for material inhomogeneity, a fiber content of 2% by volume in excess of the calculated critical fiber content has been typically used in the mix design. These decisions were made through ECC micromechanics material design theory and had been experimentally demonstrated to produce good ECC properties in previous investigations (Li et al., 2002; Kong et al., 2003-b).

3.2 Mixture Proportioning

For the present study, three different HES-ECC mixtures were produced with two different slag to Portland cement ratios (S/C) of 0.60 and 0.84 and water to cementitious material ratios (W/CM) of 0.23 and 0.34. Moreover, one mixture of a repair material (REPM) that is extensively used and widely available in the market was cast for comparison. During the production of repair material, formula provided by the manufacturer was used to arrange proportioning. To assess the bond characteristics of proposed materials, one mix of normal substrate concrete (SUBC) was cast as well. In Table 3.3, mixture proportions for three different HES-ECC mixtures and SUBC were given. During the production of HES-ECC mixtures, CEM I 52.5R high early strength Portland cement (C), ground granulated blast furnace slag (S), silica sand, expanded lightweight perlite aggregate, polyvinyl-alcohol fibers (PVA), water, high range water reducing admixture (HRWRA) and accelerating admixture (AA) were used as ingredients. In addition to fine silica sand with a maximum aggregate size (MAS) of 400 µm, pre-soaked expanded fine (with MAS of 2.0 mm) perlite aggregate was used in HES-ECC mixtures.

Table 3.3 HES-ECC and SUBC mixture proportions

Ingredients, (kg/m^3)	HES-ECC_1		HES-ECC_2		HES-ECC_3		SUBC
	Control	50%	Control	50%	Control	50%	
Total water	298	298	299	299	300	300	180
CEM I 52.5R	719	719	819	819	894	894	-
CEM I 42.5R	-	-	-	-	-	-	400
Slag	600	600	493	493	-	-	-
Coarse aggregate	-	-	-	-	-	-	920
Fine aggregate	-	-	-	-	-	-	900
Quartz sand	587	293	598	300	976	488	-
LWA (Perlite)	-	100	-	102	-	168	-
PVA fiber	26.0	26.0	26.0	26.0	26.0	26.0	-
HRWR	13.8	8.2	12.6	7.9	9.2	3.9	1.8
AA	12.3	12.3	12.3	12.3	12.3	12.3	-
AEA	-	-	-	-	-	-	0.43
Volumetric mass	2256	2057	2260	2059	2218	1892	2402
Total [W/(C+S)]	0.23	0.23	0.23	0.23	0.34	0.34	0.45
IC [W/(C+S)]*	-	0.15	-	0.16	-	0.37	-
Effective [W/(C+S)]	0.23	0.38	0.23	0.39	0.34	0.71	-
LWA/total sand	-	0.50	-	0.50	-	0.50	-
S/PC	0.84	0.84	0.60	0.60	-	-	-

*: Internal curing (IC) water to cementitious material (CM = Cement+Slag) ratio

Until desirable mortar properties are visually monitored, polycarboxylate ether type HRWRA having specific gravity of 1.1 and 40% solid content was added to the mixtures. In order to accelerate the reactions between fast setting Portland cement and water, calcium nitrate salt based set accelerator having specific gravity of 1.3 was used. PVA fibers having diameter of 39.0 μm, length of 8.0 mm, tensile strength of 1620 MPa, elastic modulus of 42.8 GPa and maximum elongation of 6.0% were added to the fresh mortar mixtures to account for the strain-hardening performance. PVA fibers were surface-coated with hydrophobic oiling agent in favor of attaining increased interfacial frictional bond between fiber and matrix instead of increasing the chemical bond between the two phases which could significantly increase the possibility of individual fibers to rupture causing loss of strain-hardening performance (Li, 1995). Expanded fine perlite aggregate (F) used in HES-ECC mixtures were with water absorption capacity of approximately 131% and specific gravity of 0.92 Along with the production of HES-ECC mixtures incorporating no saturated LWAs (control), mixtures containing and 50% of fine LWA replacements

(F_LWA), by total aggregate volume were also produced. The supplied repair material was suitable for the cases where very high early strength is required in a limited time. It is cement based with a single component incorporating fiber and polymer additives. It is rather easy to apply only by mixing water at the fraction recommended by the manufacturer. As substrate concrete (SUBC), conventional concrete which is common in the construction of rigid pavements was used. It has minimum compressive strength of 30 MPa and flexural strength of 4.5 MPa (Michigan Department of Transportation, 2009). SUBC contains a combination of fine (natural river sand with approximate particle size ranging between 0.1 and 5.0 mm) and coarse aggregates (crushed stone having maximum particle size of 12 mm). Contrary to HES-ECC mixtures, CEM I 42.5R ordinary portland cement was used in the production of SUBCs. In addition, along with air entraining admixture (AEA) for freeze thaw resistivity, HRWRA was used in SUBC mixtures for adequate consistency.

3.3 Specimen Preparation and Testing

In this study, a Hobart type mixer with 20-liter capacity was used in preparing all of the proposed mixtures. For the flexural and compressive strength characterizations of the ECC mixtures, 360×50×75 mm prism specimens and 50 mm-cube specimens were prepared, respectively. All specimens were demolded after 24 hours. The specimens were then air cured at 50±5 % RH, 23±2 ^{o}C until the day of testing. Compressive and flexural characteristics were evaluated at the end of 6 hours, 24 hours, 7 days and 28 days. Specimens prepared to be used in the characterization of mechanical properties were stored in plastic bags at 95 ± 5% RH, 23 ± 2 ^{o}C until the testing ages (see Figure 3.4).

3.3.1 Compressive Strength

Twenty four cubic samples six of which to be tested at the end of 6 hours, 24 hours, 7 days and 28 days were produced from all of the proposed mixtures. The compression test was carried out on the cubic specimens by using a 3000 kN capacity testing machine in accordance with ASTM C39 (2003) (Figure 3.5).

Figure 3.4 Moist curing of specimens to be used in mechanical property characterization after production

Figure 3.5 Compression testing machine and cubic samples

3.3.2 Flexural Performance

Flexural parameters were measured by using four-point bending tests performed on a closed-loop controlled material test system with a loading rate of 0.005 mm/s. The flexural loading was applied from span length of 304 mm and central span length of 101 mm. During the flexural tests, the load and mid-span deflection were recorded on a computerized data recording system (Figure 3.6).
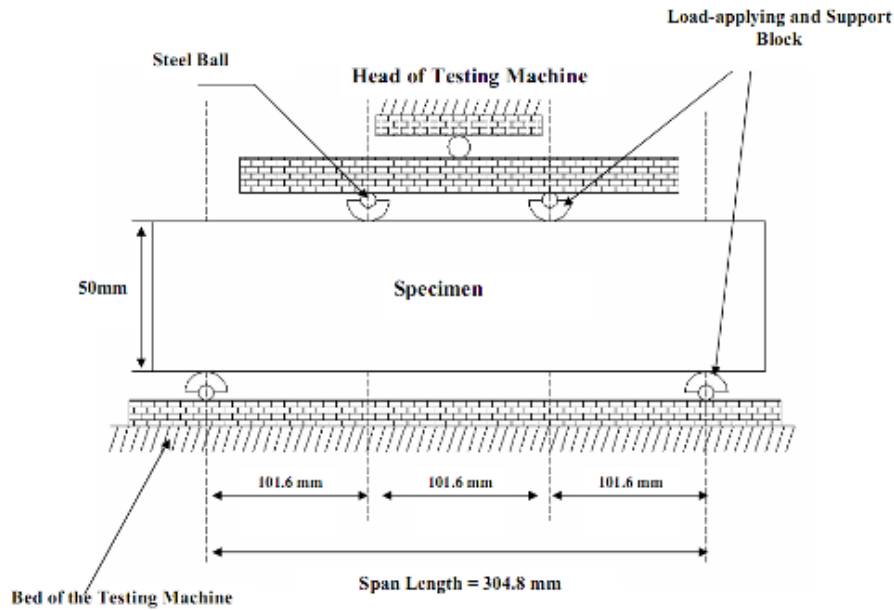
Figure 3.6 Four point bending test setup for flexural performance

The flexural deflection capacity of specimens was measured with the help of a LVDT placed on the test set-up. In the flexural stress–deformation curves, the maximum stress is defined as the flexural strength (modulus of rupture — MOR), and the corresponding deflection is defined as the flexural deformation capacity. To measure the flexural performance of mixtures, twenty four prismatic samples (6 specimens to be tested after 6 hours, 24 hours, 7 days and 28 days) having dimensions of 360x75x50 mm were cast.

3.3.3 Autogenous Shrinkage

Linear prismatic molds, also called as shrinkage drains, were used while taking autogeneous shrinkage measurements (Figure 3.7). The drains were composed of inner and outer molds. The inner mold, which was embedded inside the outer mold, measured 1000×60×90 mm.
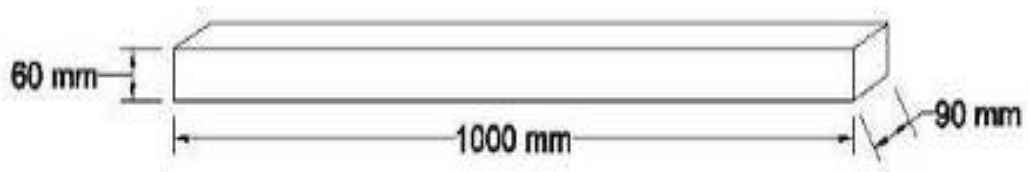
(a) Inner mold
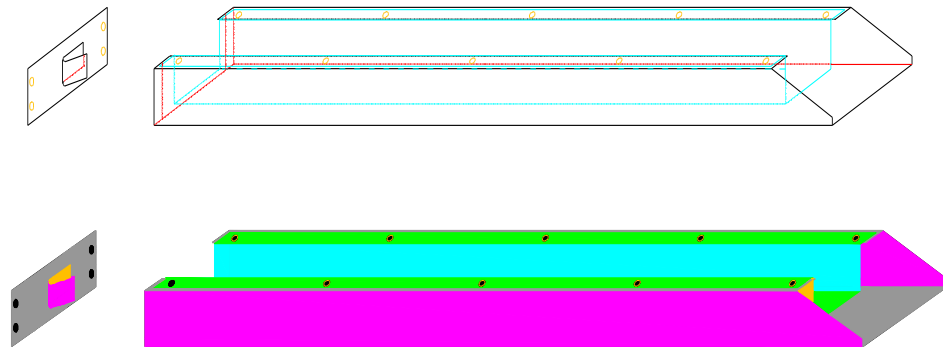
(b) Outer mold and metal plate
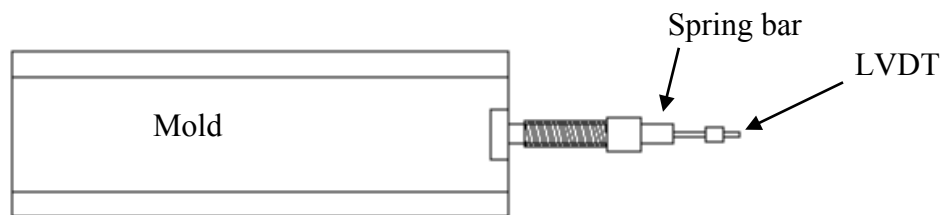
(c) Mold, LVDT and spring bar

Figure 3.7 Schematic illustration of autogenous shrinkage drain

In order to prevent friction inside the inner mold, the surfaces were covered with teflon sheets. The drains had two ends, one of which was closed and the other was free to move with an attached LVDT to measure instantaneous length changes in time. In addition to the LVDT, each drain had its own supplementary thermocouple placed between the inner and outer molds to measure temperature changes. Before placing fresh mixtures inside the drains, aerosol teflon was sprayed over the teflon cover and the inner mold of the drains was completely covered with stretch wrap (see Figure 3.8).

(a)	**(b)**

Figure 3.8 View of autogenous shrinkage test set-up a) during the preparation b) during the autogenous shrinkage test

This was done so mixtures were entirely isolated from the environment to better investigate the sole influence of hydration processes on autogeneous shrinkage of mixtures. Once the placement of fresh mixtures was completed, the top surface of the drains was covered with previously placed stretch wrap and an additional teflon sheet. LVDT measurements were started after the setting time of the mixtures was reached; until this time only temperature changes were recorded. Since it is not always easy to estimate the time needed for different mixtures to set, a common time interval was used for all mixtures. The time needed for LVDT measurements to begin was based on the period in which maximum heat liberation was observed, which worked out to two hours for all mixtures. All of the drains were kept in laboratory conditions at 23±2 °C, and 50±5% RH. The changes in LVDT and temperature measurements were recorded by a data acquisition system every 10 minutes for one week.

3.3.4 Slant Shear Test

Slant shear test method as described by ASTM C 882 (1983) has become a widely accepted test and has been adopted by numerous international codes for the evaluation of bond characteristics. Following the test procedures, proposed repair materials were bonded to the substrate concrete with elliptical slanted surface inclined at an angle of 30° from the loading axis to create cylinder specimens with the dimensions of Ø100×200 mm. During the preparation of specimens, firstly

several cylindrical specimens measuring Ø100×200 mm were cast using substrate concrete. (Figure 3.9-a).

<p align="center">(a)   (b)</p>
<p align="center">(c)   (d)</p>
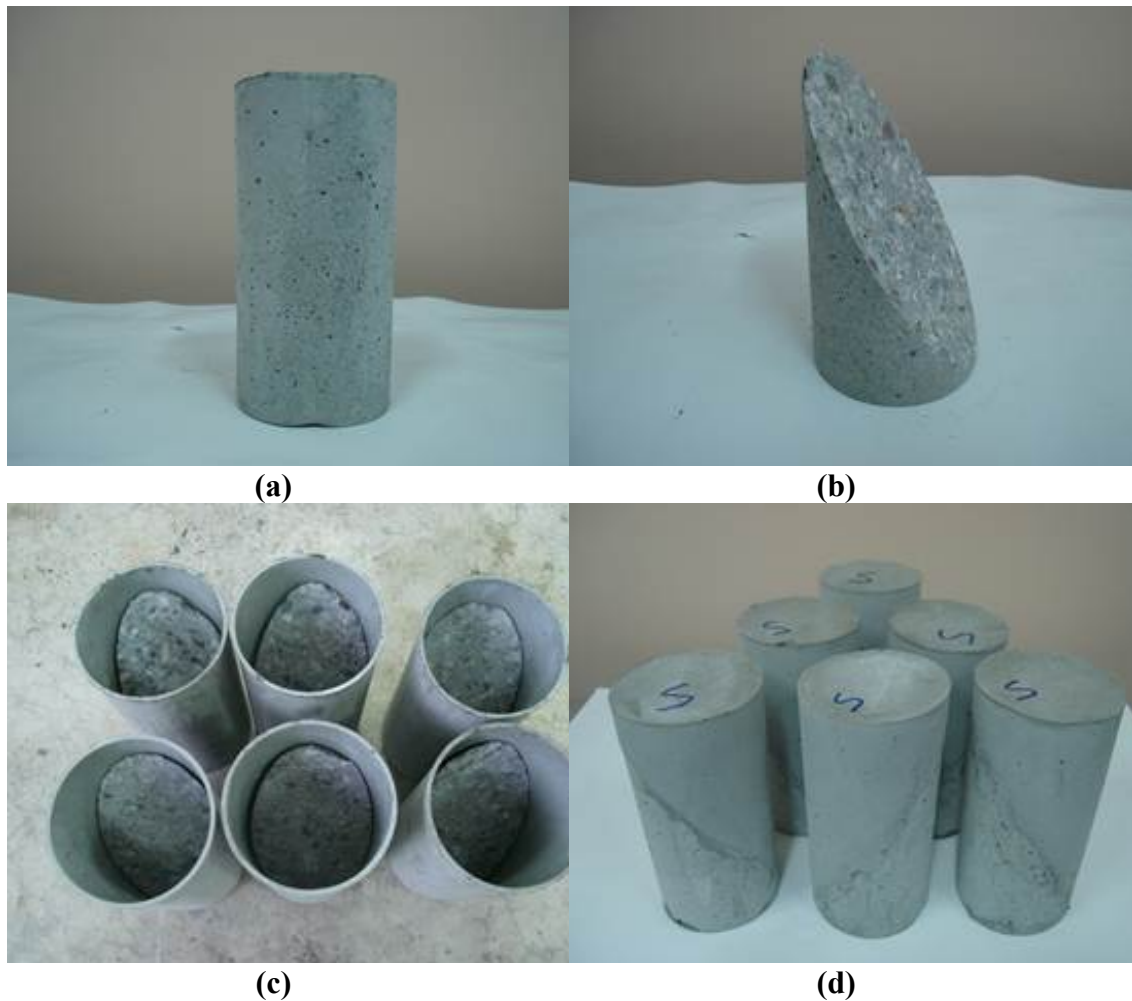
Figure 3.9 Representative preparation of composite cylinders for slant shear test

After the substrate specimens are removed from the molds, they were exposed to air curing at 23±2°C, 50±5% RH in laboratory medium for a year. Prior to placing proposed materials over the substrate concrete, special attention was paid on the age difference between the two layers in order not to encounter difficulties related to shrinkage formation in the substrate concrete and to better simulate the field conditions. After a year of air curing in the laboratory medium, half-cylinders were cut out of the whole cylinder specimens. A smooth diamond saw bond plane was used to ensure that mechanical interlock induced by rough bond plane would not affect the measured bond strength value. In Figure 3.9-b, an example of halved substrate concrete with a smooth surface prepared for the slant shear tests was

shown. After that the prepared half of the substrate concretes was inserted inside the plastic molds with their slant side up for the casting of proposed materials (Figure 3.9-c). Throughout the slant shear tests no bonding agent was used before the casting of new materials over the substrate concrete. The molds were then filled with the new materials and the composite specimens were removed from the molds after 24 hours and subjected to moisture curing in plastic bags at 95±5 % RH, 23±2°C until the predetermined testing ages. In Figure 3.9-d, composite specimens that are ready to be used for slant shear tests were shown. Twelve composite specimens four of which to be tested at the end of each 1, 7 and 28 days were produced in total for each type of proposed materials. Before the slant shear tests, all of the specimens were capped with sulfur to provide parallel surfaces and make sure the load was applied uniformly.

3.3.5 Direct Pull-Off Test

Direct pull-off tests were performed according to ASTM D 4541 (1992) standard. To be used in these tests, firstly unreinforced substrate concrete with the dimensions of 750×500×80 was cast. One day after the casting of slabs, the molds were removed and substrate concrete was kept in laboratory medium at 23±2°C, 50±5% RH for a year of duration in order not to have problems with the excessive forces that might arise due to continuing shrinkage especially at the early ages after the new materials are applied over them. When the substrate slabs have reached to a year of age, casting surface of the substrate slabs were treated with a wire brush to remove any free particles, oils, grease or surface laitance and cleaned with water afterwards. Special attention was paid not to roughen the slab surfaces up. Each big slab was divided into four equal spaces with the help of wooden molds (Figure 3.10-a) and in each free space, a different mixture of proposed materials (HES-ECCs and REPM) was cast with the thickness of 30 mm (Figure 3.10-b). During the application of new materials over the substrate concrete no bonding agent was used. Once the casting of new materials is finished, composite systems were completely isolated from the outdoor environment by plastic sheets until the commencement of core drilling process (Figure 3.10-c). The cores were started to be drilled after the final set of the mixtures was reached (Figure 3.10-d). In this study, diameter of the cores was 50 mm

with the drilling depth into the substrate concrete of nearly 15±5 mm which are common values to be applied (Austin et al., 1995).

(a)

(b)

(c)

(d)

(e)

(f)

(g)

(h)
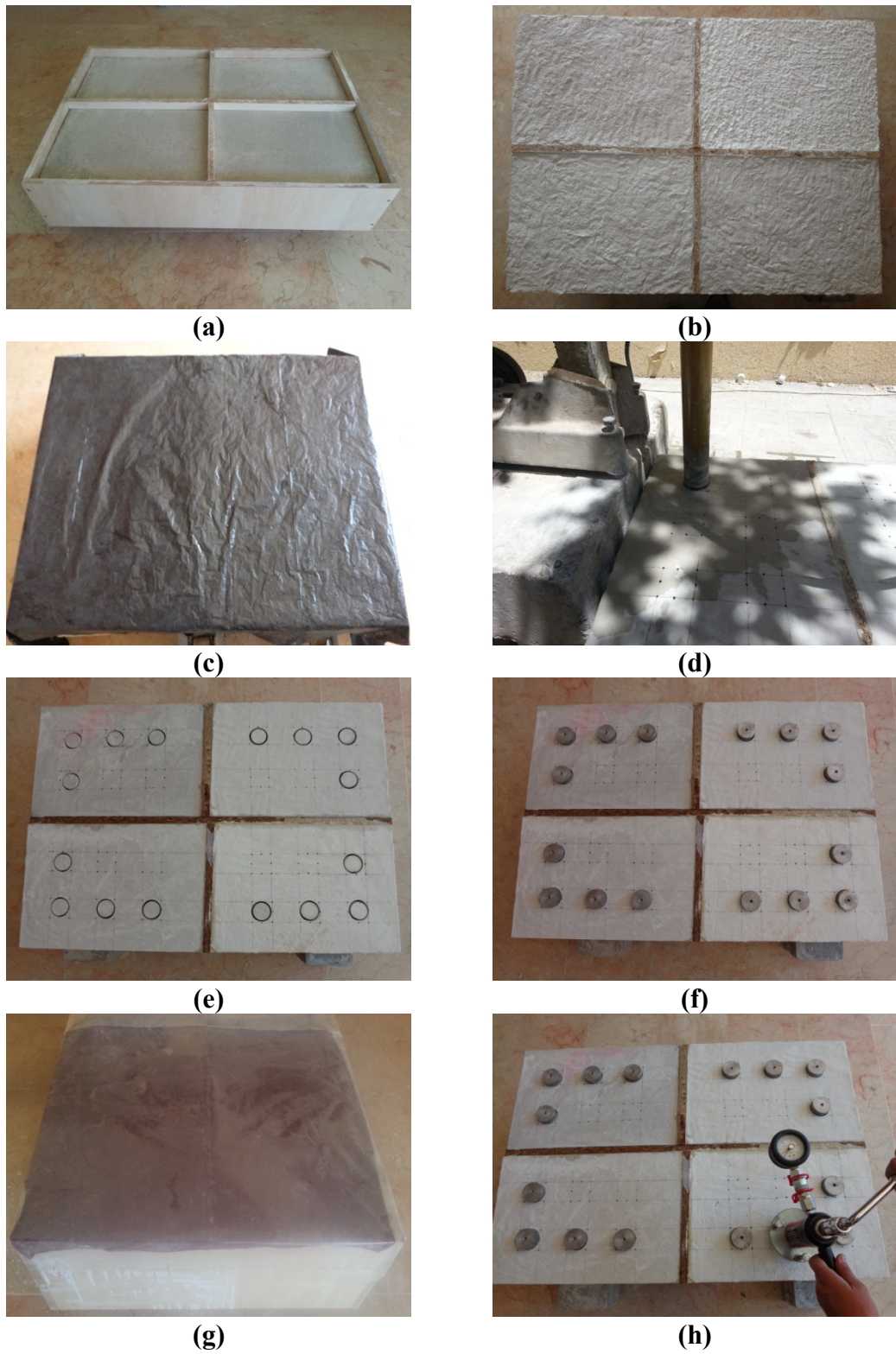
Figure 3.10 Representative preparation, curing and testing of core specimens throughout the direct pull-off tests

Care was taken to leave adequate spaces while drilling the cores since the vibration caused due to cutting drill tool can be influential on the bond strength results of adjacent cores (Figure 3.10-e). Another point that should not be overlooked is that the cores must be drilled exactly perpendicular to the overlay surface to minimize the eccentricities which may significantly change the overall bond strength results. With the completion of core drilling process, the core samples were dried and cleaned by pressurized air. Loading fixtures (metal disks) were then glued over the individual core samples with the help of an epoxy resin (Figure 3.10-f). Failure observed between the metal disks and the surface of repair materials is called as adhesive failure. This type of failure observed in the epoxy resin should occur rarely. Therefore, to increase the adherence of the disks to the core samples, bottom surface of the disks were circularly grooved to increase the contact area between epoxy resin and metal disks and not to face often adhesive failure occurrences. After the metal disks were placed and the epoxy resin was hardened, composite specimens were covered by wet burlap sacks until the testing ages (Figure 3.10-g). By this way specimens were not exposed to drying actions which could substantially increase the shrinkage-originated deformation. Direct pull of tests were performed after 1, 7 and 28 days as in slant shear tests and for each date six core samples were tested (Figure 3.10-h). During the direct pull-off tests, testing apparatus with a reaction frame was attached to the metal disks with the help of a pull pin and a precise alignment of the reaction frame was made in order to apply direct tensile loading without any eccentricity. Application of the tensile load was made at a constant pace rate until the failure of specimens. Finally, bond strength results and fracture locations of the specimens were recorded.

CHAPTER 4

RESULTS AND DISCUSSIONS

4.1 Basic Mechanical Properties

Before the commencement of bond strength tests, some of the basic mechanical properties of proposed materials (HES-ECCs and REPM) were evaluated such as compressive strength, flexural strength – modulus of rupture (MOR) and mid-span beam deflection. Compressive strength tests were performed on cubic specimens with the dimensions of 50 mm. For flexural strength tests prism specimens having 360×75×50 mm dimensions were produced. The tests were performed by using twenty four prism specimens for flexural tests and twenty four cubic specimens for compressive strength tests at the ages of 6 hours, 24 hours, 7 days and 28 days. After the completion of casting of specimens for compression and flexure, they were kept in the molds and covered with plastic burlaps at 23 ± 2°C for 24 hours, and subsequently stored in plastic bags at 95±5% RH, 23±2°C until the pre-determined testing ages. For the measurement of flexural parameters, four-point bending tests were carried out on a closed-loop controlled material test system with a loading rate of 0.005 mm/s. The span length of the flexural loading was 304 mm and the central span length was 101 mm. During the flexural tests, the load and mid-span beam deflection were recorded on a computerized data recording system. The flexural deflection capacity of specimens was measured with the help of a LVDT placed on the test setup. In the flexural stress-deformation curves, the maximum stress is defined as the flexural strength (modulus of rupture — MOR), and the corresponding deflection is defined as the flexural deformation capacity.

In Table 3, compressive strength results of the HES_ECCs and REPMs calculated in compliance with ASTM C39 were tabulated.

Table 3.4 Mechanical properties and autogenous shrinkage of REPM and HES-ECC mixtures

Mixture ID		Compressive strength (MPa)				Flexural strength (MPa)				Mid-span beam deflection (mm)				Autogenous shrinkage (με)		
		6 h.	24 h.	7 d.	28 d.	6 h.	24 h.	7 d.	28 d.	6 h.	24 h.	7 d.	28 d.	24 h.	7 d.	28 d.
HES-ECC_1	Control	26.9	64.4	85.0	95.1	8.0	9.5	10.9	11.1	3.6	2.7	1.4	1.0	1336	1627	2101
	F_50%	22.0	47.2	73.9	82.5	7.9	8.9	10.1	11.3	3.7	3.3	2.6	2.4	360	802	899
HES-ECC_2	Control	33.6	68.4	84.8	93.0	8.7	10.0	11.0	12.5	2.8	2.0	1.4	1.2	1271	1471	1911
	F_50%	28.3	51.3	67.7	78.4	7.8	9.1	9.5	11.5	3.7	3.1	2.4	2.2	432	796	944
HES-ECC_3	Control	29.6	56.2	64.6	75.7	7.2	8.6	10.0	10.2	2.3	1.9	1.2	1.0	666	706	858
	F_50%	19.0	36.5	47.1	51.2	6.2	6.9	8.6	9.5	3.4	2.9	2.4	2.2	-113	-140	-18
REPM		21.9	45.1	68.5	76.0	5.1	5.7	7.7	8.1	0.57	0.45	0.38	0.31	98	96	104

42

Each data presented in the table was calculated by taking average of six cubic specimens. Improvement in the compressive strength results showed great variation depending on different factors such as the type of binder, W/CM ratio, and dosage used.

When the six-hour compressive strength results of control specimens are compared it can be seen that HES-ECC_2 specimens with 33.6 MPa was the highest in ranking which was followed by HES-ECC_3 and HES-ECC_1 control specimens with the values reaching up to 29.6 MPa and 26.9 MPa, respectively. Irrespective of the mixture type, results have continuously increased until the end of 28 days of age though the increasing trend was less visible beyond 24 hours due to the diminishment in hydration kinetics with time. It should be pointed out that despite the similarities (same W/CM ratio of 0.23) in mix proportioning of HES-ECC_1 and HES-ECC_2 control mixtures there is nearly a 25% of difference in 6-hour compressive strength results which is in close relation with the changes in S/C ratios (from 0.84 to 0.60). Therefore, the reason for HES-ECC_2 control specimens to show higher compressive strength results could be due to higher tricalcium silicate (C_3S) and tricalcium aluminate (C_3A) amounts that are two governing compounds influencing the formation of calcium silicate hydrate (C-S-H) gels. Moreover, with the reduction in S/C ratio, the paste of HES-ECC_2 control specimens gets denser since the particle size of CEM I 52.5R Portland cement (460 m^2/kg) is finer in comparison to slag (425 m^2/kg). Along with the filler effect, the higher fineness and particle surface area of CEM I 52.5R Portland cement provide more nucleating sites and OH^- ions as well as alkalis into the pore fluid (Li and Zhao, 2003). The influence of W/CM ratio on compressive strength results can be more understandable by comparing the results of HES-ECC_2 and HES-ECC_3 mixtures so that a small increase in W/CM ratio from 0.23 to 0.34 leaded the results to decrease nearly by 12% although S/C ratio dropped significantly from 0.60 to 0.00. This shows that W/CM ratio is a much better bench mark of defining the changes in compressive strength results. It is believed that saturated LWAs would contribute to fasten the hydration reactions and lead higher strength achievements (Lura et al., 2004). Although it seems to be realistic, addition of saturated LWAs did not have the anticipated influence over compressive strength results. For example, addition of saturated LWAs into the mixtures instead of quartz sand caused overall 6-hour compressive strength results to decrease by

18%, 16% and 35% for HES-ECC_1, HES-ECC_2 and HES-ECC_3 mixtures, respectively. This finding is associated with the interruption of PVA fibers to disperse uniformly in the matrices by coarser LWAs compared to silica sand. As the fibers were prevented to distribute uniformly, they start to form bundles behaving like voids in the cementitious matrices. Moreover, the addition of coarser LWAs may lead the regional water to cementitious materials ratio in the interfacial transition zone to increase and consequently overall compressive strength results to decrease (Mehta and Monteiro, 2006). As it is also seen from Table 3.4, 6-hour compressive strength of REPM is 21.9 MPa which is lower than all HES-ECC mixtures excluding HES-ECC_3 specimens with 50% of LWA replacement with a minor difference. Although the results show variations, the minimum 6-hour compressive strength values of all the proposed materials in this study is more than enough to satisfy the minimum values stated by different authorities for fast repair applications (FHWA, 1999; Anderson, 2001).

The flexural strength test results of HES-ECCs and REPM were provided in Table 3.4. Each data given in the table was found by averaging six different prismatic specimens. According to the table, the highest MOR attainment was captured by HES-ECC_2 control specimens with 8.7 MPa at the end of six hours. The same values were 8.0, 7.2 and 5.1 MPa for HES-ECC_1, HES-ECC_3 control and REPM specimens, respectively. It can be seen from Table 3.4 that regardless of the mixture type, the increase in MOR values with time is not that of sudden as in compressive strength results which may be attributed to more complicated material properties that could affect MOR values such as tensile strain capacity, tensile first cracking strength, and ultimate tensile strength (Qian, 2009). The replacement of saturated LWAs with the quartz sand resulted in reductions in MOR values without any regard to the mixture type and age. This trend of the HES-ECC mixtures incorporating saturated LWAs was correlated with inconvenience of individual fibers to be coated by the matrix itself. It should be stated here that although HES-ECCs incorporating pre-soaked LWAs exhibited lower MOR values compared to control mixtures, the minimum MOR value at the end of six hours which was obtained from HES-ECC_3 mixture with saturated LWAs (6.2 MPa) was greater than the value obtained from REPM and minimum values reported by several authorities (FHWA, 1999; Anderson, 2001).

Ultimate mid-span deflection values which can be accepted as a measure of materials' ductility were presented in Table 3.4. When the mid-span beam deflection results of HES-ECC_1 and HES-ECC_2 mixtures are compared, it can generally be said that at the same W/CM ratio, specimens having lower S/C ratio (HES-ECC_2) resulted in lower values. The probable reasons for HES-ECC_2 specimens to show lower results compared to HES-ECC_1 mixture was found to be attributable to higher fracture toughness, bond strength and friction between the HES-ECC_2 matrix and the fibers. The lowest mid-span deflection results were obtained from HES-ECC_3 mixture having the highest W/CM ratio of 0.34. As seen from Table 1, in HES-ECC_3 mixtures, slag was not used as a replacement of Portland cement which leaded the amount of coarser (in comparison to slag) quartz sand to increase. Thus, it may be possible that uniform distribution of fibers were interrupted due to coarser aggregate gradation of HES-ECC_3 mixtures leading insufficient coating of fibers individually and lower deflection results. With the utilization of saturated LWAs in the mixtures, mid-span beam deflection results increased significantly. This trend was found in relation with the positive effects of LWAs on the reduction of toughness values which may strongly influence the occurrence of multiple micro-cracks instead of localized cracks with larger crack widths in favor of attaining large deformability. As it is also clear from Table 3.4, the lowest mid-span deflection values were recorded from REPMs at all the ages showing considerably lower deformability of specimens under bending loading.

4.2 Slant Shear Test

The slant shear test results obtained at the end of 1, 7 and 28 days were presented in Table 3.5 along with the failure modes at the end of 28 days. Each data given in the table was found by averaging four cylindrical composite specimens and during the tests load was applied with a loading rate of 0.25 MPa/second. The bond strength obtained from slant shear tests were calculated by dividing the maximum load observed at the failure as a result of compressive loading by the elliptical area of the bonded interface. The average coefficient of variation (COV) from all the tests was lower than 5% level showing the consistency of the values.

Table 3.5 Slant shear bond strength test results and failure modes

Mixture ID.		Bond Strength (MPa)			Failure Mode
		1 day	7 days	28 days	28 days
HES-ECC_1	Control	8.4	22.9	24.2	All through substrate
	F_50%	5.5	17.6	20.8	
HES-ECC_2	Control	9.2	24.0	25.6	All through substrate
	F_50%	7.5	20.0	23.8	
HES-ECC_3	Control	7.1	17.0	20.8	All through substrate
	F_50%	4.7	15.7	19.0	
REPM		6.9	18.0	21.6	2 through slanted interface 2 through a monolithic rupture
ACI bond strength range		2.8 to 6.9	6.9 to 12.4	13.8 to 20.1	-

When the results of HES-ECC control specimens are considered, it can be seen from Table 3.5 that, highest bond strength was achieved by HES-ECC_2 control specimens with 9.2 MPa at the end of one day. HES-ECC_2 control specimens were followed by HES-ECC_1 and HES-ECC_3 control specimens with the values reaching up to 8.4 and 7.1 MPa levels, respectively. Probable reasons for HES-ECC_2 control specimens to show higher bond strength results were associated with the factors influencing compressive strength results which were discussed previously in detail. For a better simulation, compressive strength results were plotted versus bond strength values in shear and the relationship between them was investigated (Figure 3.11).
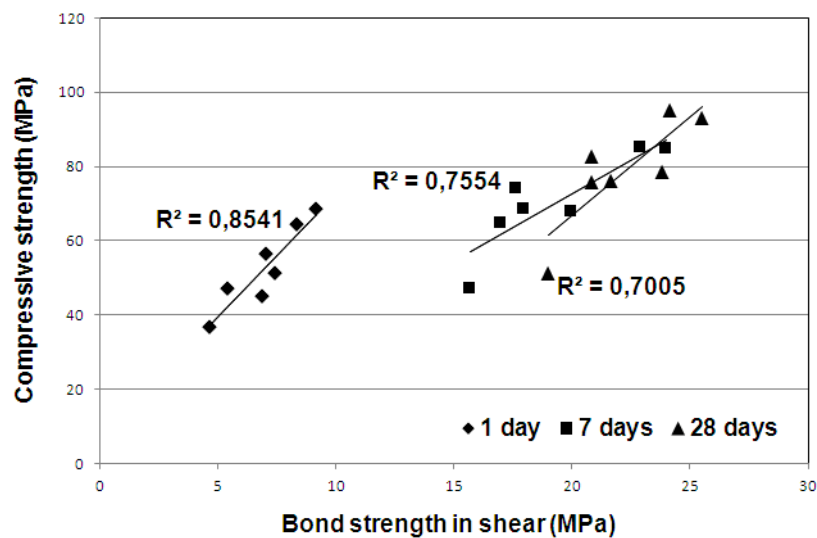

Figure 3.11 Relationship between compressive strength and slant shear bond strength at different ages

For example, while correlation coefficient (R) was 0.92 in the case of 1-day-old specimens, the same value was 0.87 for 7-day-old and 0.84 for 28-day-old specimens. In other words, while 85% of the variation in the results was accounted for by the linear relationship in the case of 1-day-old specimens, 76% and 70% of the variation was accounted for by 7 and 28-day-old specimens, respectively.

Another noticeable point in the bond strength results was that the values showed an increasing trend until the end of 28 days irrespective of the mixture type. The increasing trend in the bond strength results was found to be unexpected since the differential shrinkage (autogenous shrinkage in this case) between the new material and substrate concrete increases with time (Table 3.4) creating detrimental tensile forces near the slanted interfaces. The explanation for the contradictory results could be that with the application of compressive loading during the slant shear tests, tensile stresses were easily eliminated and as the differential shrinkage increased, the corresponding failure load to overcome the exerted tensile forces increased as well leading final bond strength results to improve at later ages (Santos and Julio, 2011). This therefore implies that bond strength results in terms of slant shear tests were better simulated by the changes in compressive strength values as compared with differential shrinkage formation. The increase in the results was however more rapid between the ages of 1 and 7 days. For example, while the bond strength results of HES-ECC_2 control specimens increased by 162% between the 1th and 7th days, this value was found to be %6 between the ages of 7 and 28 days. This behavior of the specimens was correlated with the deceleration of hydration reactions with time. The replacement of fine silica sand with saturated LWA had a great influence on bond strength measurements. While saturated LWA usage was expected to internally cure the densely packed matrix of HES-ECC mixtures and lead enhanced bonding properties, bond strength results decreased as silica sand was replaced by the saturated LWA. As seen from Table 3.5, the addition of saturated LWA caused the bond strength values of 1-day old control specimens to drop approximately 35%, 19% and 34% for HES-ECC_1, HES-ECC_2 and HES-ECC_3 mixtures, respectively. Same modality was true for 7 and 28-day-old specimens as well. By considering abovementioned approach, it may be concluded that lower tensile forces created due to reduced differential shrinkage formation leaded the corresponding failure load and relatedly the bond strength results in shear to be lower. Moreover,

the inclusion of coarser LWAs into ultrafine system of HES-ECCs may cause reductions in the contact area between the substrate and new material which is the place for chemical reactions to take place. Therefore, the possibility of smaller particles such as slag and cement to fit in inside the pores existing in the interfaces were reduced with the utilization of considerably coarser LWAs which most probably led to interruptions in mechanical interlocking and intermolecular forces. Another possible reason that might be responsible for the reductions in the bond strength results with the addition of saturated LWAs could be the formation fiber bundles which act like pores in the matrix itself especially the ones near the slanted shear surfaces. The bond strength results of REPM which was produced as an alternative to HES-ECC mixtures were found to be in the mid-range at the end of all specified curing ages as seen from Table 3.5 Although, the bond strength results varied significantly depending on the mixture types, all of the results either satisfied or exceeded the values given by the Concrete Repair Guide (2004) which specifies a bond strength range for selecting repair materials in accordance with slant shear test results.

Along with the bond strength results, failure modes of proposed materials at the end of 28 days were also presented in Table 3.5. This was done to understand whether the failure occurred along the shear planes or if the cylinders were failed due to severe cracking in new material or substrate concrete. As seen from the table, all of the HES-ECC mixtures failed through the substrate concrete regardless of the mixture type. However, in the case of REPM, while half of the specimens showed interface debonding, the other half showed monolithic rupture type which extends through both new material and substrate concrete together (Figure 3.12).

Substrate failure type which observed in all of the HES-ECC specimens is highly desirable since it shows that existing substrate concrete is the weakest part of the composite system. The reason for HES-ECC specimens to show better performance in terms of slant shear bond strength results could be related with the very high binder amount in the HES-ECC mixtures which might significantly increase the chance for calcium hydroxide in the substrate concrete to participate in secondary hydration reactions to create additional C-S-H gels. This might have led the

microstructure of the interface between the HES-ECC and SUBCs to be improved substantially in comparison to REPMs.

(a) **(b)**

Figure 3.12 Failure modes of HES-ECC and REPM specimens at the end of 28 days as a result of slant shear tests

4.3 Direct Pull-off Test

The bond strength values obtained as a result of direct pull-off tests and the failure modes of core samples were given in Table 3.6.

Table 3.6 Tensile pull-off bond strength test results and failure modes

Mixture ID.		Bond Strength (MPa)			Failure Mode
		1 day	7 days	28 days	28 days
HES-ECC_1	Control	1.93	1.85	1.79	All through substrate
	F_50%	2.12	2.18	2.22	
HES-ECC_2	Control	2.13	2.07	1.98	All through substrate
	F_50%	2.45	2.53	2.64	
HES-ECC_3	Control	1.83	1.81	1.87	All through substrate
	F_50%	1.93	2.05	2.11	
REPM		1.51	1.54	1.72	2 through slanted interface 2 through a monolithic rupture

The results were obtained at the end of 1, 7 and 28 days by taking average of six different specimens. As seen from the table, depending on the curing time, mixture

type and LWA replacement, bond strength results of all proposed materials ranged between the values of 1.51 and 2.64 MPa. Although, some of the control specimens (HES-ECC_1 and HES-ECC_2) behaved differently, all the mixtures in general showed increasing trend in bond strength results with time. The addition of saturated LWA into HES-ECC control mixtures caused a significant increase in bond strength results. For example, at the end of one day, pull-off bond strength results of HES-ECC_1 control specimens increased from 1.93 to 2.12 MPa level with the addition of saturated LWAs. The same was true for the rest of HES-ECC control mixtures at the end of each time period. The increasing trend in tensile bond strength results with the addition of saturated LWA might be of relevance with the amount of HRWRA used in the mixtures. As seen from Table 3.1, the amount of HRWRA was significantly reduced in HES-ECCs since surface areas of the mixtures decreased with the incorporation of saturated LWAs. This might have led HES-ECCs having saturated LWAs to have more concentrated packing of hydration products in the interfaces and stronger bonds. The increase in bond strength results of HES-ECC specimens with time was however less evident in the case of HES-ECC_3 mixture. This behavior of HES-ECC_3 specimens was surprising since the addition of saturated LWAs leaded the HES-ECC_3 control mixtures to swell which would result in the occurrence of beneficial compressive stresses near the interface areas. It therefore appears that although low shrinkage formation is a favorable characteristic for the attainment of bond with high quality, uniform distribution of fibers and ductility of the mixtures seem to have greater influence on bond strength results obtained by tensile pull-off testing. As can be seen from Table 3.1, there is no slag incorporation in HES-ECC_3 mixtures which causes the sand amount to increase significantly in comparison to other HES-ECC mixtures. It seems that increase in sand amount caused non-uniform distribution of fibers due to coarser particle size distribution and the interruption of uniform fiber distribution was even more exacerbated with the addition of saturated LWAs. Therefore, it can be stated that although HES-ECC_3 mixtures were with the lowest differential shrinkage formation, lower ductility which was originated due to non-uniform distribution of PVA fibers leaded weak planes near the interfaces. However, due to better fiber distribution and higher ductility in the case of HES-ECC_1 and HES-ECC_2 mixtures, higher deformations caused due to differential shrinkage were easily accommodated which might have had slight influence on the interfaces and leaded higher bond strength results.

When HES-ECC mixtures and REPM are compared, it can be seen that the bond strength results of REPM were markedly lower than any HES-ECC mixture regardless of the time of testing despite significantly low differential shrinkage formation of REPM specimens. The reason for HES-ECC mixtures to show higher bond strength results compared to REPM could be associated with the influence of PVA fibers on interfaces along with the higher ductility of HES-ECCs. In this regard it may be stated that fibers play an important role in lowering total shrinkage-related deformation at the interfaces and lead more uniform distribution of microcracks by arresting, blunting, deflecting and branching them. As the size of flaws is reduced at the interfaces, repair assembly can resist to a higher tensile loading. Here one can understand that not the magnitude of total deformation but the ability of any repair material to easily bear large strain formations should be accounted for during the decision making of a suitable material.

The relationship between compressive strength and bond strength values obtained as a result of tensile pull-off testing was given in Figure 3.13.
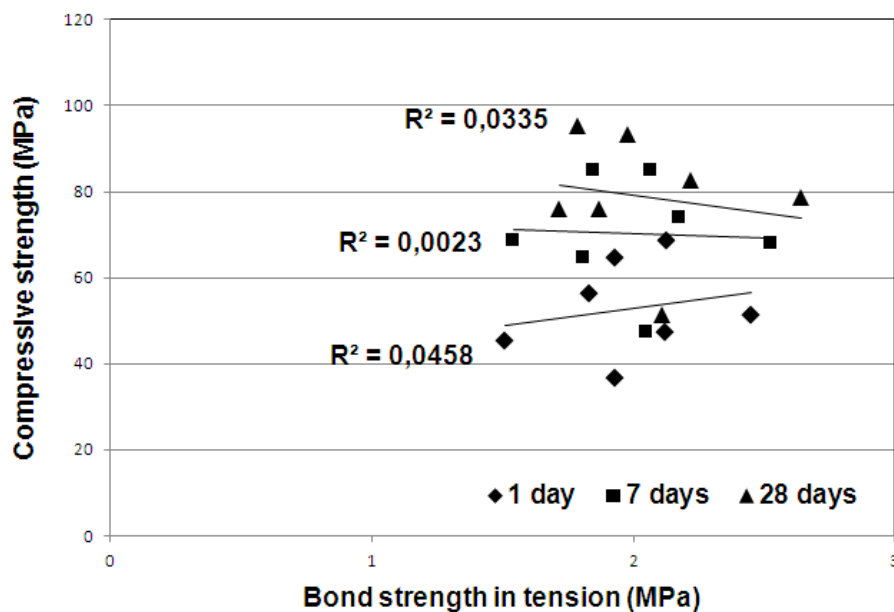

Figure 3.13 Relationship between compressive strength and tensile pull-off bond strength at different ages

When the mixtures are examined individually it seems that compressive strength is not an influential parameter for tensile bond strength development which is in line with what was stated in the literature (Bonaldo et al., 2005). As seen from the figure,

51

irrespective of the time of testing, there is a large scattering between the two parameters and correlation coefficients of specimens are rather low indicating high variability of results as opposed to slant shear tests. This finding may be associated with the complexity of repair-bond behavior in the case of direct pull-off tests. Average COV values obtained from all the pull-off tests were lower than 10% level which was higher compared to slant shear test results. Higher variation in pull-off test results which were believed to be observed due to several factors such as differential shrinkage, assumption of perfect testing conditions, effect of fiber distribution which is impossible to assure equally and varying mixture compositions make the tensile bond strength results difficult to correlate with mechanical properties such as compressive strength.

In Table 3.6, failure modes of proposed materials at the end of 28 days were given. As previously discussed larger scattering in tensile bond strength results (COV<10%) were observed compared to slant shear test results (COV<5%). Partly, this was originated due to the variability in bond nature and partly, this was because of the differences in the testing procedures. In a repair assembly, failures can be seen at the substrate, at the interface, at the newly applied repair material or at epoxy used to attach the disk to the core. The failure may also occur as a combination of the failure modes described above. The failure observed at the substrate concrete provides actual measurement of the bond strength and shows that the repair assembly can be regarded as adequate. Other failure types only provide lower bound measurements since the bond stays untouched. As seen from Table 3.6, almost all of the six specimens tested in the case of all HES-ECC mixtures failed from the SUBC. In the case of REPM, almost all failure types were monitored (Figure 3.14).

However, only one out of six cores showed substrate failure type. The probable reasons that might contribute to the occurrence of desired failure types and higher tensile bond strength results in the case HES-ECC mixtures were discussed previously and will not be further explained here. It should be stressed out that although the failure modes show variation depending on the mixture type, bond strength values of all HES-ECC mixtures are in the range of very good to excellent bond strength levels according to Sprinkel and Ozyildirim (2000) while REPM specimens show bond strength levels between good and very good.
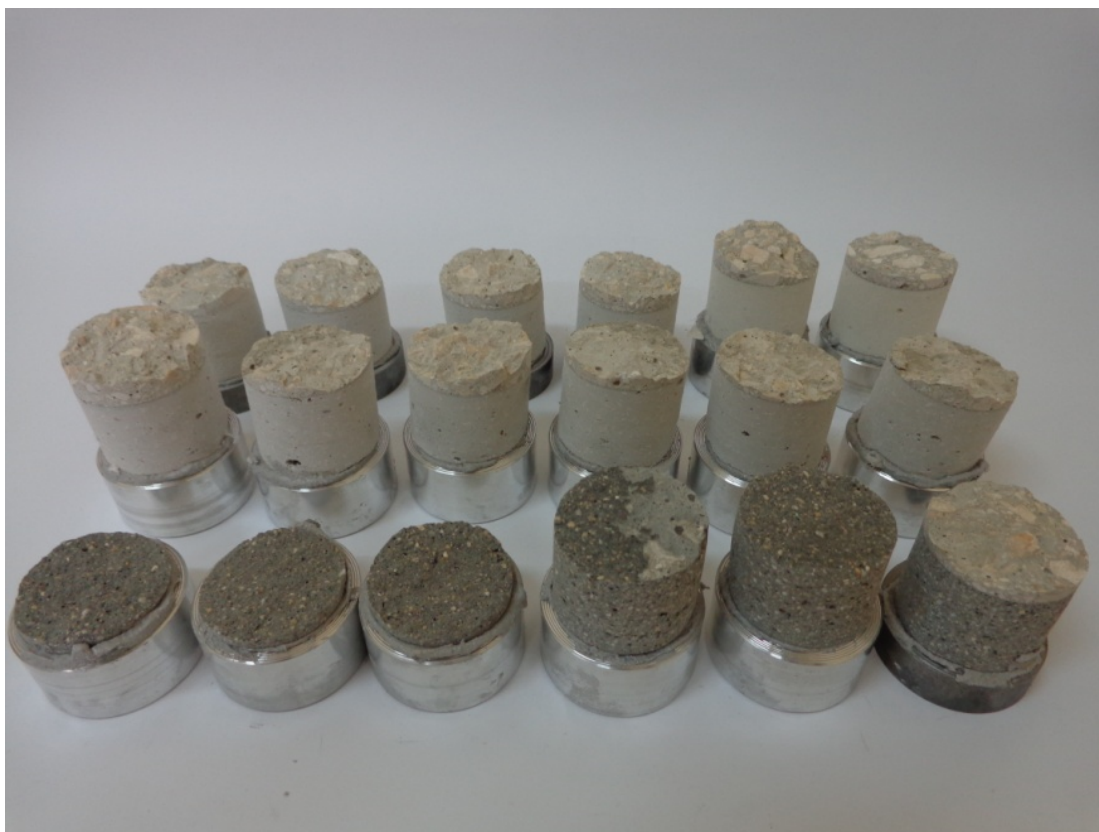
Figure 3.14 Failure modes of HES-ECC and REPM specimens at the end of 28 days
as a result of direct pull-off tests

4.4 Correlation Between Slant Shear and Direct Pull-off Tests

Conflicting arguments are available in the literature related to the correlation of results between shear and tension tests. According to Delatte et al. (2000-a), average ratio of shear bond results to tension bond results is 2.0. Silfwerbrand (2003) states that there is a ratio between torsional shear bond strength and tensile pull-off strength in the range 2 to 3. In another study, bond strength results obtained from slant shear tests were linearly correlated with the pull-off bond strength results with a correlation coefficient of approximately 0.95 (Julio et al., 2004). Although all of the cited studies are unarguably of great value, all of the specimens proposed throughout this study behaved in a completely different manner. Relationship between slant shear and direct pull-off test results were displayed in Figure 3.15.
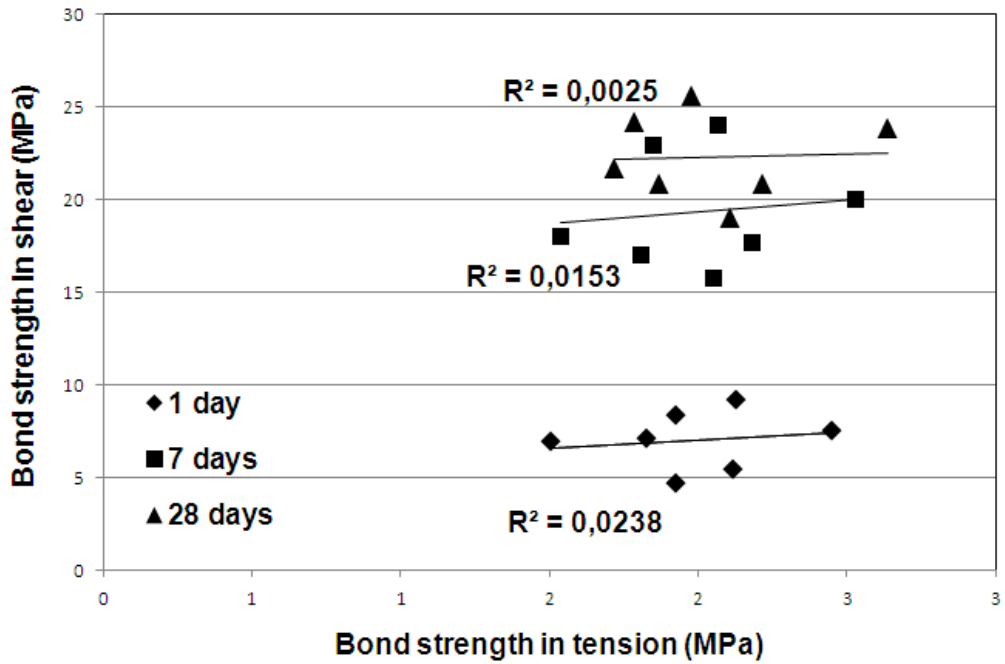
Figure 3.15 Correlation between slant shear and direct pull-off test results

As it is clear from the figure, the results obtained from both bond tests did not show a consistent correlation regardless of the time of testing so that R values for 1, 7 and 28 days were 0.15, 0.12 and 0.05, respectively. As it can be deduced from the studies exemplified above, interface shear strength and tensile bond strength results may show significant variations since the results of both tests are strongly influenced by several parameters such as specimen size, magnitude of differential shrinkage, loading rate, testing apparatus and so on. Therefore, having an exact correlation between both tests is highly questionable due to tremendous differences between the natures of the tests and further research is needed on related subject for better understanding.

CHAPTER 5

CONCLUSIONS

This paper presents and analyses the results of an experimental research by aiming at investigating the bond characteristics of newly developed HES-ECC and commercially available REPM in terms of slant shear and tensile pull-off tests. For the investigation, HES-ECC mixtures with two different W/CM (0.23 and 0.34) and S/C (0.60 and 0.84) were produced along with an extensively used REPM. During the production of HES-ECCs saturated fine LWAs were added to the mixtures with the purpose of lowering the differential shrinkage formation and improving ductility. Control specimens with no LWA replacements were produced for comparison as well. In addition to basic mechanical properties, the influence of compressive strength and differential shrinkage on the bond performance of proposed materials was discussed and the results obtained from both bond tests were compared. Following conclusions were drawn

- It can be stated that there is a linear relationship between compressive strength and bond strength results in shear although the correlation between the two parameters weakens in time. It seems differential shrinkage does not have significant effect on slant shear test results since shrinkage-originated deformation is easily eliminated by the compressive loading applied during the tests. While all of HES-ECC mixtures showed substrate failure, half of REPMs failed from interface and half of them failed monolithically at the end of 28 days.

- Based on the experimental results, it can be concluded that compressive strength is not a decisive parameter for tensile bond strength formation. Utilization of saturated LWAs significantly increased the tensile bond strength results of HES-ECC mixtures which is related to lower shrinkage and higher ductility of mixtures incorporating LWAs. Tensile bond strength of all HES-ECC mixtures was substantially higher than that of REPMs

55

although REPMs show significantly lower shrinkage formation which indicates the importance of ductility in repair applications. Almost all of HES-ECC specimens failed from SUBC while REPMs exhibit nearly all failure types at the end of 28 days.

- Results obtained from both tests show that no correlation exists between slant shear and direct pull-off tests which is associated with the factors affecting completely different tests.

REFERENCES

ACI Committee 546.(2004). Concrete Repair Guide, 546R-04.

Ali, Y. A. Z. and Ambalavanan, R. (1999). Flexural behavior of reinforced concrete beams repaired with styrene-butadiene rubber latex, silica fume and methylcellulose repair formulations. *Magazine of Concrete Research*, **51** (2), 113-120.

Anderson, J. (2001). Paving repair finds a four-hour champion. *Concrete Construction*, **46** (12), 69-70.

ASTM C 882-78. (1983). Standard test method for bond strength of epoxy resin systems used with concrete, American Society for Testing and Materials, Philadelphia, PA.

ASTM C39.(2003). Standard test method for compressive strength of cylindrical concrete specimens.American Society for Testing and Materials.West Conshohocken, PA, USA.

ASTM C89.(2009). Standard specification for slag cement for use in concrete and mortars.American society for testing and materials.West Conshohocken, PA, USA.

ASTM D4541-92.(1992). Standard test method for pull-off strength of coatings usingportable adhesion testers.American society for testing and materials.

Austin S., Robins P. and Pan Y. (1999). Shear bond testing of concrete repairs. *Cement and Concrete Research*, **29**, 1067–1076.

Austin, S., Robins, P. and Pan, V. (1995).Tensile bond testing of concrete repairs.*Materials and Structures*, **995** (28), 249–59.

Beushausen, H. and Alexander, M. G. (2008).Bond strength development between concretes of different ages.*Magazine of Concrete Research*, **60**, 65–74.

Bonaldo, E., Barros, J. A. O. and Lourenço, P. B. (2005).Bond characterization between concrete substrate and repairing SFRC using pull-off testing.*International Journal of Adhesion and Adhesives,***25**, 463–74.

Chen, P., Fu, X. and Chung, D. D. L. (1995).Improving the bonding between old and new concrete by adding carbon fibres to the new concrete.*Cement and Concrete Research*, **25** (3), 491–496.

Delatte, N. J., Wade, D. M. and Fowler, D. W. (2000-b). Laboratory and field testing of concrete bond development for expedited bonded concrete overlays. *ACI Materials Journal*, **97** (3), 272–280.

Delatte, N. J., Williamson, M. S. and Fowler, D. W. (2000-a). Bond strength development of high-early-strength bonded concrete overlays. *ACI Materials Journal*, **97** (2), 201–207.

El-Rakib, T. M., Farahat, A. M., El-Degwy, W. M. and Shaheen, H. H. (2003). Shear transfer parameters at the interface between old and new concrete. *ICPCM Proceedings*, Cairo, Egypt.

Emberson, N. K. and Mays, G. C. (1990). Significance of property mismatch in the patch repair of structural concrete. Part 1: properties of repair systems. *Magazine of Concrete Research*, **42** (152), 147–160.

Emmanuel, B. O. A., Lev, K. and Leslie, T. G. (1998).Mechanistic-based model for predicting reflective cracking in asphalt concrete overlaid pavements.*Transporation Research Record,***1629**, 234–241.

Emmons, P. H. (1994). Concrete repair and maintenance illustrated: problem, analysis, repair strategy and techniques, pp. 155-164.

Fe´de´rationInternationale de la Pre´contrainte (1978). Shear at the Interface of Precast and In-Situ Concrete. FIP, Lausanne, Technical report.

Federal Highway Administration (FHWA), Manual of Practice.(1999). Materials and procedures for rapid repair of partial-depth spalls in concrete pavements, 135 pp.

Hassan, K. E., Brooks, J. J. and Al-Alawi, L. (2001).Compatibility of repair mortars with concrete in a hot-dry environment.*Cement and Concrete Composites*, **23**, 93-101.

Julio, E. S., Branco, F., Silva, V. D., and Lourenço, J. F. (2006). Influence of added concrete on concrete-to-concrete bond strength. *Building and Environment*, **41**(12), 1934-1939.

Julio, E., Branco, F. and Silva, V. D. (2004).Concrete-to-concrete bond strength.Influence of the roughness of the substrate surface.*Construction and Building Materials*, **18**, 675–81.

Kamada, T. and Li, V. C. (2000). The effects of surface preparation on the fracture behavior of ECC/concrete repair system. *Cement and Concrete Composites,* **22** (6), 423–431.

Kim, Y. Y., Kong, H. J. and Li, V. C. (2003).Design of Engineered Cementitious Composite (ECC)suitable for wet-mix shotcreting.*ACI Materials Journal,* **100,** 511-518.

Knofel, D. and Wang, J. F. (1994). Properties of three newly developed quick cements. *Cement and Concrete Research*, **24** (5), 801-812.

Kong, H. J., Bike, S. and Li, V. C. (2003-a).Development of a Self-Consolidating Engineered Cementitious Composite Employing ElectrostericDispersion/Stabilization.*Journal of Cement and Concrete Composites*, **25,** 301-309.

Kunieda, M. and Rokugo, K. (2006).Recent progress on HPFRCC in Japan.*Advanced Concrete Technology*,**4,** 19-33.

Larralde, J., Elpert, M. S. and Weckermann, D. A. (2001). Simplified shear test for the adhesion of FRP composites to concrete. *Cement, Concrete and Aggregates*, **23** (1), 66–70.

Lepech, M. D., and Li, V. C. (2008).Large-scale processing of engineered cementitious composites.*ACI Materials Journal*, **105** (4), 358-366.

Li, G. and Zhao, X. (2003). Properties of concrete incorporating fly ash and ground granulated blast-furnace slag. *Cement and Concrete Composites*, **25**, 293-299.

Li, G., Xie, H. and Xiong, G. (2001). Transition zone studies of new-to-old concrete with different binders. *Cement and Concrete Composites*, **23** (4-5), 382-387.

Li, M. (2009).Multi-scale design for durable repair of concrete structures, Ph.D. Dissertation, University of Michigan, 2009, 425 pp.

Li, M. and Li, V. C. (2011). High-early-strength engineered cementitious composites for fast, durable concrete repair — material properties. *ACI Materials Journal*, **108** (1), 3.

Li, S. E., Geissert, D. G., Frantz, G. C. and Stephens, J. E. (1999).Freeze–thaw bond durability of rapid-setting concrete repair materials.*ACI Materials Journal*, **96** (2), 241–249.

Li, V. C. (1997). Engineered cementitious composites tailored composites through micromechanical modeling. *Fiber Reinforced Concrete: Present and the Future*, Banthia, N. A., Bentur and Mufti, A. Editor, pp. 64-97.

Li, V. C. (1998). Engineered cementitious composites tailored composites through micromechanical modeling, in: N. Banthia, A. Bentur, A. Mufti (Eds.), *Fiber Reinforced Concrete: Present and the Future*, Canadian Society for Civil Engineering, pp. 64-97.

Li, V. C. (2003). On engineered cementitious composites (ECC): A review of the material and its applications. *Advanced Concrete Technology*, **1**, 215-230.

Li, V. C. and Leung, C. K. Y. (1992). Theory of steady state and multiple cracking of random discontinuous fiber reinforced brittle matrix composites. *ASCE Journal of Engineering Mechanics*, **118,** 2246–2264.

Li, V. C., Mishra, D. K. and Wu, H. C. (1995). Matrix Design for Pseudo Strain-Hardening Fiber Reinforced Cementitious Composites.*RILEM Journal of Materials and Structures*, **28,** 586-595.

Li, V. C., Wang, S. and Wu, C. (2001). Tensile Strain-hardening Behavior of PVA-ECC. *ACI Materials Journal,* **98,** 483-492.

Li, V. C., Wu, C., Wang, S., Ogawa, A. and Saito*,* T. (2002).Interface tailoring for strain-hardening PVA–ECC, *ACI Materials Journal,* **99** (5), 463–472.

Lim, Y. M. and Li, V. C. (1997). Durable repair of aged infrastructures using trapping mechanism of engineered cementitious composites. *Cement and Concrete Composites,* **19** (4)*,* 373–385.

Lin, Z. and Li, V. C. (1997). Crack bridging in fiber reinforced cementitious composites with slip-hardening interfaces. *Mechanics and Physics of Solids,* **45**,763-787.

Lin, Z., Kanda, T. and Li, V. C. (1999). On interface property characterization and performance of fiber reinforced cementitious composites. *Concrete Science and Engineering,* **1**, 173-184.

Lura, P., Bentz, D. P., Lange D. A., Kovler, K. and Bentur, A. (2004)., Pumice aggregates for internal water curing, *PRO 36: Proceedings of the International RILEM Symposium on Concrete Science & Engineering* - A Tribute to ArnonBentur, RILEM Publications S.A.R.L., 137-151.

Marshall, D. B. and Cox, B. N. (1988). A J-integral method for calculating steady-state matrix cracking stresses in composites. *Mechanics of Materials*, **8,** 127–133.

Mather, B. and Warner, J. (2004). Why do concrete repairs fail, interview held at University of Wisconsin, Department of Engineering Professional Development, Wis. http://aec.engr.wisc.edu/resources/rsrc07.html>.

Mehta, P. K. and Monteiro, P. J. M. (2006). Concrete: Structure, Properties, and Materials. Third Edition, McGraw Hill, New York.

Michigan Department of Transportation, (2009).MDOT Bridge Design Manual.

Momayez, A., Ramezanianpour, A. A., Rajaie, H. and Ehsani, M. R. (2004).Bi-surface shear test for evaluating bond between existing and new concrete.*ACI Materials Journal*, 99-106.

Neville A. M. (2002). Properties of Concrete, Fourth Edition, Pearson Education, London.

Oluokun, A. F. and Haghayeghi, A. R. (1998). Flexural behavior of reinforced concrete beams retrofitted or repaired with slurry infiltrated mat concrete. *ACI Structural Journal,* **95** (6), 654-664.

Parker, F. and Shoemaker, M. L. (1991).PCC pavement patching materials and procedures.*Journal Materials in Civil Engineering*, **3** (1), 29-47.

Pigeon, M. and Saucier, F. (1992).Durability of repaired concrete structures.*Proceedings of an International Symposium on Advances in Concrete Technology*, Athens, pp. 741–773.

Qian, S. (2007). Influence of concrete material ductility on the behavior of high stress concentration zones. PhD thesis, University of Michigan, Ann Arbor, USA.

Qian, S., Zhou, J., De Rooij, M. R., Schlangen, E., Ye, G. and Van Breugel, K. (2009).Self-healing behavior of strain hardening cementitious composites incorporating local waste materials, *Cement and Concrete Composites*, **31**, 613-621.

Robins, P. J. and Austin, S. A. A. (1995).Unified failure envelope from the evaluation of concrete repair bond test.*Magazine of Concrete Research*, **47** (170), 57–68.

Russell, H. G. (2004). Concrete bridge deck performance.*Transportation Research Board National Research.*

Sahmaran, M., Yucel, H. E., Yildirim, G., Al-Emam, M. and Lachemi, M. (2013).Investigation of bond between concrete substrate and ECC overlays.*Journal of Materials in Civil Engineering*, Accepted for publication.

Santos, P. M. D. and Julio, E. N. B. S. (2011). Factors affecting bond between new and old concrete. *ACI Materials Journal*, **108** (4), 449-456.

Seehra, S. S., Gupta, S. and Kumar, S. (1993). Rapid setting magnesium phosphate cement for quick repair of concrete pavements – characterization and durability aspects. *Cement and Concrete Research,* **23** (2), 254-266.

Silfwerbrand, J. (2003). Shear bond strength in repaired concrete structures. *Materials and Structures*, **36**, 419– 424.

Souza, R. H. F. and Appleton, J. (1997). Flexural behavior of strengthened reinforced concrete beams, *Materials and Structures,***30**, 154 – 159.

Sprinkel, M. M and Ozyildirim, C. (2000). Evaluation of high performance concrete overlays placed on Route 60 over Lynnhaven Inlet in Virginia. Final report, Virginia Transportation Research Council, Charlottesville, Virginia.

Sprinkel, M. M. (1998). Very-early-strength latex-modified concrete overlay, Report No. VTRC99-TAR3, Virginia Department of Transportation, Richmond, Virginia, 11pp.

Stang, H. and Li, V. C. (1999).Extrusion of ECC-material.*In Proceedings Of High Performance Fiber Reinforced Cement Composites 3(HPFRCC 3)* edited by H. Reinhardt and A. Naaman, Chapman & Hull, pp. 203-212.

Tayeh, B. A., Abu Bakar, B. H., Johari, M. A. M. and Voo, Y. L. (2012). Mechanical and permeability properties of the interface between normal concrete substrate and ultra high performance fiber concrete overlay. *Construction and Building Materials,***36**, 538–548.

Tschegg, E. K., Ingruber, M., Surberg, C. H. and Munger, F. (2000). Factors influencing fracture behaviour of old–new concrete bonds. *ACI Materials Journal*, **97** (4), 447–453.

Uherkovich, I. (1994). Questions concerning long-time behavior of concrete repair, in: F.H. Wittmann (Ed.), Adherence of Young on Old Concrete, *AEDIFICATIO*, 177 – 181.

United States Department of Transportation (USDT) (2000). Tensile bond strength of a high performance concrete bridge deck overlay. Federal Highway Administration MCL Project 9904, Washington, Field Test Report.

Wang, S. and Li, V. C. (2004).Tailoring of pre-existing flaws in ECC matrix for saturated strain hardening.*Proceedings of FRAMCOS-5*, Vail, Colorado, USA, pp. 1005–1012.

Wang, S. and Li, V. C. (2006). High early strength engineered cementitious composites. *ACI Materials Journal*, **103** (2), 97-105.

Weimann, M. B. and Li, V. C. (2003). Hygral behavior of engineered cementitious composites (ECC).*International Journal for Restoration of Buildings and Monuments*, **9**, 513-534.

Yucel, H. E., Jashami, H., Sahmaran, M., Guler, M. and Yaman, I. O. (2013). Thin ECC overlay systems for rehabilitation of rigid concrete pavements. *Magazine of Concrete Research*, **65** (2), 108–120.

Zhang, J. and Li, V. C. (2002). Monotonic and fatigue performance in bending of fiber reinforced engineered cementitious composite in overlay system. *Cement and Concrete Research,***32** (3), 415–423.